https://doi.org/10.5194/egusphere-2022-1165
Preprint. Discussion started: 14 November 2022

Real-time measurements of NMVOCs in the central IGB, Lucknow, India: Source characterization and their role in O_3 and SOA formation

Vaishali Jain[1], Sachchida N. Tripathi[1,2], Nidhi Tripathi[3], Mansi Gupta[3], Lokesh K. Sahu[3], Vishnu Murari[1], Sreenivas Gaddamidi[1], Ashutosh K. Shukla[1], Andre S.H. Prevot[4]

[1]Department of Civil Engineering, Indian Institute of Technology Kanpur, Kanpur, 208016, India
[2]Centre for Environmental Science and Engineering, Indian Institute of Technology Kanpur, Kanpur, 208016, India
[3]Space and Atmospheric Sciences Division, Physical Research Laboratory, Ahmedabad, 380009, India
[4]Laboratory of Atmospheric Chemistry, Paul Scherrer Institute, 5232, Switzerland

Correspondence to: Dr Sachchida N. Tripathi (snt@iitk.ac.in), Dr. Lokesh K. Sahu (Lokesh@prl.res.in)

Abstract: Lucknow is the capital of India's largest state, Uttar Pradesh, one of South Asia's most polluted urban cities. Tropospheric photochemistry relies on non-methane volatile organic compounds (NMVOCs), which are ozone and secondary organic aerosol precursors. Using the proton-transfer reaction time of flight mass spectrometer (PTR-ToF-MS) at an urban background site in Lucknow, the chemical characterisation of NMVOCs was performed in real-time from Dec-2020- May 2021. The campaign mean concentrations of the NMVOCs were 125.5 ±37.5 ppbv. The average concentrations of NMVOCs are relatively high during winter. An advanced multi-linear engine (ME-2) model was used to perform the NMVOCs source apportionment using positive matrix factorisation (PMF). It resolves the five main sources contributing to these organic compounds in the atmosphere. They include traffic, two solid fuel combustion factors, secondary volatile organic compounds and volatile chemical products. Biomass burning contributes most to the NMVOCs and SOA formation, while interestingly, traffic sources most influence ozone formation. Significant differences in the composition of the two solid fuel combustion indicate the influence of local emissions and transport of regional pollution to the city. The high temperature during summer leads to more volatilisation of oxygenated VOCs.

1. Introduction

Non-methane volatile organic compounds (NMVOCs) are carbon-containing gaseous compounds in the troposphere. NMVOCs can have significant effects (direct and indirect) on human health and the environment. These compounds have a half-life ranging from hours to months (Atkinson*, 2000). Exposure (Inhalation or direct contact) to high levels of NMVOCs can produce multiple chronic and acute health effects on humans, including nose, eyes, throat, and liver irritation. NMVOCs like benzene, acrolein, and aromatic amines are carcinogens subject to long-term exposure (Balakrishnan et al., 2015; WHO, 2021).

The NMVOCs in the atmosphere act as precursors of ozone (O_3) and secondary organic aerosols (SOA) (Hallquist et al., 2009; Monks et al., 2015). They are oxidised by primary oxidant radicals such as hydroxyl radicals (OH), chlorine (Cl), and nitrate (NO3) in the presence of nitrogen oxides (NOx) and sunlight and can lead to the formation of ozone near the surface (Atkinson et al., 2004; Carter, 1994) and also secondary oxygenated volatile organic compounds (OVOCs) (de Gouw et al., 2005). These OVOCs undergo further oxidation, gaining polar functional groups or oligomerise and becoming less volatile. When these compounds have sufficiently low vapour pressures, these products may condense to form a particle-phase secondary organic aerosol mass (Hallquist et al., 2009; Heald et al., 2008; Monks et al., 2009). The chemical composition of the parent compound, NOx concentrations and relative concentrations of OH and chloride radicals during the day and NO_3 during the night (Warneke et al., 2004) are factors that ultimately determine the fate of the formation of these aerosol products (Jang et al., 2002). At high NOx levels, VOCs degrade to form carbonyls, hydroxy carbonyls, organic nitrates and peroxyacetyl nitrates (PAN). In contrast, low NOx conditions tend to produce fewer volatile compounds and organic peroxides after reaction with HO2 radicals and favour SOA production from OVOCs.(Hallquist et al., 2009; Kroll et al., 2006; Ng et al., 2007; Xu et al., 2014).

The inherent complexity in the non-linear VOCs-NO_X-O_3 relationship and change in ozone levels as a function of VOCs and NOx is understood by ozone isopleths. When VOCs are relatively high, and NOx is

https://doi.org/10.5194/egusphere-2022-1165
Preprint. Discussion started: 14 November 2022

relatively low, ozone production is limited by NOx, which is considered a NOx-sensitive regime. Conversely, when VOCs are relatively low, and NOx is high, ozone production is determined by the concentration of VOCs and considered as VOC- sensitive regime (also known as a NOx-saturated regime) (Chameides et al., 1992). It is observed that the urban area of Delhi was frequently associated with VOC-sensitive chemical regimes (Sharma and Khare, 2017). The reduction of VOCs from anthropogenic emissions would reduce ozone levels more instead of reducing NOx levels. (Sharma and Khare, 2017) also simulated that reducing NOx by 50% in Delhi would increase ground-level ozone production by about 10-50%. In contrast, it is recommended that strategies control abatement measures for NMVOCs, which would effectively reduce tropospheric ozone production by 60% more than abatement of ozone or particulate matter ($PM_{2.5}$) alone.

The buildup of Surface ozone and SOA synergistically deteriorates the air quality and escalates harmful effects on humans and flora-fauna (Annenberg et al., 2018; Burnett et al., 2014; Pye et al., 2021). The increased $PM_{2.5}$ concentrations and other pollutants lead to economic and recreational loss, deterioration in the health of citizens, an increase in morbidity and premature mortality risks, and biodiversity loss. Extreme haze events are one of the major challenges for Indian cities, being among the most air-polluted cities in the world. Despite their importance, the spatial and temporal variability of the concentrations of NMVOCs, which are precursors to secondary organic aerosols and ozone, remain unknown for most Indian cities. The lack of identification of their sources and relative contribution remains a challenging task for policy-driven measures.

The development and evolution of strategies need an understanding of the seasonal and temporal variations and sources of NMVOCs. The reaction pathway is different for different NMVOCs and depends on the reaction rates of the species. Therefore, the ozone formation potential (OFP) of all NMVOCs is not the same. NMVOCs are categorised into distinct families based on their chemical structure and mass/charge (m/z) ratios. Some of these NMVOCs have lower OFPs than others and tend to form less ozone in the atmosphere. Understanding these OFPs in different chemical regimes would help identify families or species of NMVOCs of greater concern for surface ozone production control.

Here, we deployed real-time instruments in Lucknow city, situated in the middle of the Indo-Gangetic plain, to understand the contribution of long-range transport and local VOC emissions. The aerosol loadings in the city have been unprecedentedly high for the last two decades (Lawrence and Fatima, 2014; Markandeya et al., 2021; Sharma et al., 2006). The $PM_{2.5}$ concentrations were found to be highest in the industrial area during winter compared to residential and commercial spaces (Pandey et al., 2013, 2012). Lucknow is one of the fastest-growing cities and is now known for its manufacturing, commercial and retail hub. The exploding population due to increased migration from nearby towns and villages have widened the city boundaries. The number of registered personal motor vehicles in the city as of 2017 is about ~2 million (Government of India, 2019), that had been increasing at an average rate of 9% every year since 2007. Increased industrial and construction activities, unregulated energy and fuel consumption, unchecked vehicular pollution and unsustainable urbanisation are major driving forces for poor air quality in Lucknow (Uttar Pradesh Pollution Control Board, 2019). Nevertheless, minimal work has been carried out to investigate air pollution and its health impacts in the city, most of which are focused on particulate pollution. To our knowledge, there are no reported measurements of NMVOCs over the city.

This study discusses the first measurements of NMVOCs using PTR-ToF-MS over the crucial site in the middle of the Indo-Gangetic basin (IGB). This study focuses on the relative source contribution of the detected NMVOCs using positive matrix factorisation and their associations with organic aerosols. A specific goal of this study is to distinguish between primary emissions and secondary formations of VOCs. Moreover, the contribution of sources of NMVOCs towards ozone and secondary organic aerosol formation is also estimated.

2. Methodology

2.1. Sampling site description

Lucknow, also known as the 'City of Nawabs', is situated in the centre of the Indo-Gangetic Basin. It is an urban city located on the banks of the Gomati River and is the state capital of Uttar Pradesh, India. Currently, the city has two major Indian National Highways (NH-24 and NH-30) interjecting. The city has 125 petrol/diesel filling stations and seven designated industrial areas (*Brief Industrial Profile of District Lucknow, Uttar Pradesh*, 2018). Besides this, 255 brick kilns operate within and around Lucknow city. Only ~4.7% of the area of the district is covered by forest area with ~ 2.8 million population (Census of India, 2011). The city has eight large-scale, public-sector undertakings, eleven medium-scale industries, and hundreds of MSMEs (*Brief Industrial Profile of District*

https://doi.org/10.5194/egusphere-2022-1165
Preprint. Discussion started: 14 November 2022

Lucknow, Uttar Pradesh, 2018). Most industrial and manufacturing plants are related to steel metal components and fabrication, automobile parts, chemical industries, food and agro-based and handicraft sectors (chikankari, zardozi, bone craft). The Industrial map of Lucknow and nearby districts with major/mini-industrial areas, large/medium scale industries, sewage treatment plants, solvent based industries, sugar mills, pharmaceutical industries, and power plants are shown in Figure 1.

The sampling site (26° 51' 55.4" N, 81° 0' 17.5" E) is marked as a red triangle in Figure 1. It is located in Lucknow city at a height ~12 m above the ground in of Uttar Pradesh Pollution Control Board (UPPCB) office building in Gomti Nagar. The sampling site is surrounded by residential buildings, office complexes, schools, big parks and commercial spaces. The measurements of NMVOCs were conducted using a proton-transfer-reaction time-of-flight mass-spectrometer (PTR-TOF-MS, Ionicon Analytik GmbH). The instrument's inlet is connected to a Teflon PFA (perfluoroalkoxy) tube (1.5m in length) for drawing air samples at the flow rate of 60mL/min. The sampling was conducted from 18th December 2020 to 5th May 2021, covering three seasons: winter, spring, and summer. The gaps in the sampling period from 3-8th January and 21st March - 9th April are due to maintenance and calibration of the instrument. The average daily temperature is ~28 ºC over the city. The pre-dominant wind direction is South, southeast during colder and southwest during warmer periods, as shown in supplementary Figure S1. The wind speed is relatively calm during winters than in summers. All the instruments were placed inside a temperature-controlled laboratory during the campaign. Detailed descriptions of the instruments can be found in subsequent sections.

2.2. Instrumentation and data analysis

The PTR-TOF-MS is widely used for measuring NMVOCs with high mass resolution and sensitivity. A detailed description of the instrument can be found in other studies (Graus et al., 2010; Jordan et al., 2009; Tripathi et al., 2022; Tripathi and Sahu, 2020), while a brief description is given here. The PTR-TOF-MS is based on the chemical ionisation method, facilitated by proton-transfer reactions with hydronium (H_3O^+) ions as the primary reactant ion, which causes much less fragmentation of organic molecules in the sampled air. The natural components of air (nitrogen, oxygen, hydrogen, carbon dioxide, Argon etc.) have a lower proton affinity than water molecules. They thus do not react with H_3O^+, while most VOCs have higher proton reactivity than water, facilitating non-dissociative proton transfer. These H_3O^+ ions are generated with high efficiency (~99.5%) through a hollow cathode discharge source, and then these reactant ions enter the adjacent drift tube section. The sampled air is also injected into the drift tube section, where proton transfer reactions between hydronium ions $[H_3O^+]$ and neutral VOCs $[R_iH_j]$ occur to form protonated product VOC ions $[R_iH_{j+1}]$, and water molecules $[H_2O]$ as shown in equation 1. These $[R_iH_{j+1}]$ then enter the orthogonal acceleration reflectron time-of-flight mass spectrometer via a specially designed transfer lens system (Jordan et al., 2009).

$$H_3O^+ + R_iH_j \rightarrow R_iH_{j+1} + H_2O \quad (1)$$

The parameters of the drift tube of the instrument were maintained at 2.2-2.4 mb, 60º C, 600 V, 130 Td for pressure, temperature, voltage and electric field (E/N; where E = electric field strength and N= gas number density) respectively and operated with a time resolution of 30 seconds. Typically, these or similar values have been observed as most suitable for ambient air measurements of NMVOCs (Blake et al., 2009, 2004). The PTR-ToF-MS can identify hydrocarbons (HC) and oxygenated VOCs at sub-ppbv levels within a second (Graus et al., 2010; Müller et al., 2012). In this study, the PTR-ToF-MS measured 173 NMVOC ions (m/z 31.018 to 197.216) at the sampling site. To compute the concentrations of VOCs, a typical value of 2 x 10^{-9} cm^3 s^{-1} of the proton transfer reaction rate coefficient (Smith and Spanel, 2005) has been employed. The calibration of the instrument was performed at the starting, middle and end of the campaign using a certified standard gas mixture (L5388, Ionicon Analytik GmbH Innsbruck, with a stated accuracy better than 8%) containing ~1.0 ppmv of VOCs. A detailed description of the similar set-up and unit is given in the previous studies (Jain et al., 2022; Tripathi et al., 2022). The exact mass-identified chemical formula and family of species of the observed NMVOCs (173 in number) is given in supplementary Table S1. The concentrations of these measured 173 ions are averaged over the study period and compared in the box plots as shown in Supplementary Figure S2. The three most abundant NMVOC species are observed as acetaldehyde, acetone, and acetic acid.

2.3. Supporting measurements

A high-resolution time-of-flight aerosol mass spectrometer (HR-ToF-AMS, Aerodyne Research Inc., USA) was also deployed for campaign measurements. HR-ToF-MS (Decarlo et al., 2006) measures size-resolved mass

https://doi.org/10.5194/egusphere-2022-1165
Preprint. Discussion started: 14 November 2022

spectra of non-refractory $PM_{2.5}$ (NR- $PM_{2.5}$) with high time resolution (2 mins). A detailed description of the instrument can be found in other studies (Lalchandani et al., 2021; Shukla et al., 2021) and is explained briefly here. The ambient aerosols enter the aerodynamic lens through a sampling inlet (100 µm diameter critical orifice) and focus on a narrow beam. This particle beam then enters a sizing chamber, where it is sorted based on its size. This size-resolved beam enters the vaporisation chamber, and the non-refractory part of the particles (Nr-$PM_{2.5}$) vaporises at 600° C. These gaseous molecules are then ionised and detected by a ToF-MS, depending on their m/z ratio. The NR-$PM_{2.5}$ is chemically characterised by organics (Org), nitrates (NO_3), sulphates (SO_4), and chlorides (Cl). An aethalometer (Magee Scientific, model AE-33) was also deployed at the campaign site to measure the black carbon (BC) mass concentrations. The details about the instrument can be found in the previous studies (Lalchandani et al., 2021; Shukla et al., 2021). The sampling site is a part of the national central ambient air quality monitoring stations (CAAQMS). The meteorological parameters (temperature, relative humidity, wind parameters) and concentrations of trace gases (NO_2, SO_2, Ozone) are downloaded from the CAAQMS dashboard, managed by the central pollution control board (CPCB) for Gomti Nagar station.

2.4. Source apportionment

Numerous receptor models have been used to analyse the dynamic behaviour of ambient aerosol measurements and relate it to physical sources. One of the recently developed algorithms, positive matrix factorisation (PMF) (Paatero and Tapper, 1994), has been explored by numerous studies to apportion the measured bulk composition and temporal variation of aerosols (Talukdar et al., 2021; Zhang et al., 2011). The PMF algorithm is a non-negative, symmetrical factor analytic technique that produces unique factorisation by iterative reweighting of individual data values and unique solutions. It solves the common bilinear equation, given as (Eq. 2):

$$X\ (mxn) = G\ (mxp)\ F(pxn) + E \tag{2}$$

where X represents the measured matrix, G and F are unknown matrices, and E is the error/ residual matrix. The m and n represent the time series and individual mass dimensions, and p is the number of factors. The calculated quantities G and F represent timeseries and profiles of the specific factor of the model solution, respectively. The ME-2 solver decreases the rotational ambiguity and fits the G and F entries to minimise the uncertainty in quantity 'Q'. This 'Q' is the sum of the squared residuals weighted by their respective uncertainties, as given in equation 3. From the equation, it can be inferred as a normalised chi-square metric, where e_{ij} represents the residual matrix of E and σ_{ij} represents measured data uncertainties.

$$Q = \sum_{i=1}^{m}\sum_{j=1}^{n}\left(\frac{eij}{\sigma ij}\right)^2$$

$$Q_{exp} = n.m - p.(m+n) \tag{3}$$

Another quantity, Q_{exp}, degree of freedom, depends on the dimensions of the matrix and the number of factors. In an ideal case, the ratio of Q/Q_{exp} is expected to be 1, with all the elements of the measured matrix and uncertainties well-defined. However, it has been noticed in earlier studies that the absolute value of the ratio, Q/Q_{exp}, is not always equal to 1 due to errors in measured data uncertainties, transient sources, and unknown model residuals. It is recommended to use relative change in this ratio and characteristics of the physical source while choosing the optimum factor solution (Paatero and Tapper, 1994, 1993). In this study, this algorithm is applied over the measured VOCs mass spectra using ME-2 (multi-linear engine) (Paatero, 1999) over SoFi Pro (Source Finder, Datalystica Ltd., Switzerland) (Canonaco et al., 2013) in a graphical interface software Igor Pro version 6.37 (Wavemetrics, Inc., Portland). Earlier studies have applied a similar PMF algorithm over mass spectra of 90 VOCs in Delhi (Jain et al., 2022; Wang et al., 2020) and 101 VOCs in Beijing (Wang et al., 2021). In this study, for the first time, we have included 170 NMVOC ions measured by PTR-ToF-MS from m/z 42.034 to m/z 197.216. The input and residual error matrix for the PMF analysis were prepared using timeseries of mass spectra and calculated individual errors for each data point, as explained in the previous study (Jain et al., 2022). After incorporating the calibration factors, the uncertainties or residual error matrix is estimated by multiplying the peak area with the correction matrix. The total uncertainties vary in the range of 8-12% during calculations of the mixing ratio of NMVOCs. The three most abundant VOCs ions are not included in the PMF analysis due to their high signal-to-noise ratios and relatively higher concentrations than other ions, as shown in supplementary Figure S2. The pretreatment of the input matrix also includes applying a minimum error threshold. The weak variables, having a signal-to-noise ratio <2 and bad variables, having a signal-to-noise ratio <0.2, are down-weighted by 2 and 10, respectively (Paatero and Hopke, 2003; Ulbrich et al., 2009). The optimum factor solution from the PMF analysis was chosen as explained in section 3.2 and correlated to external measurements (Org, NO_3,

https://doi.org/10.5194/egusphere-2022-1165
Preprint. Discussion started: 14 November 2022

SO_4, Cl from Nr-$PM_{2.5}$, organic resolved factors, gases (O_3, NO, NO_2, NOx, SO_2), temp, RH, WD, WS, and BC concentrations).

2.5. Ozone formation potential and SOA yield of NMVOCs

Ozone formation potential (OFP) is a reactivity-based estimation technique to assess the sensitivity of the VOCs for ozone formation (e.g., (Tripathi et al., 2021)). The ground-level ozone is produced by photochemical reactions involving VOCs and NO_X. The non-linear dependence of ozone formation on the concentrations of NO_X and VOCs are described empirically by the ozone isopleths. Most Indian cities have high NOx concentrations and lie in VOCs-sensitive regimes, i.e., oxidation of VOCs produces more radicals initiating ozone formation. Numerous VOCs are emitted into the atmosphere from various sources, followed by distinct reaction pathways and have different OFPs. The calculated reactivities of VOCs have been investigated in multiple computer modelling studies depending on the environmental conditions (Carter, 1994). This approach is based on calculating OFP on maximum incremental reactivity (MIR) for individual VOC species, as given in the equation 4. Here, this equation is adopted and modified (Carter, 2010, 1994) to calculate the ozone formation potential for each of the factors, resolved from PMF analysis as given below (Eq. 4),

$$OFP(i) = \sum_{j=0}^{n} [VOC_j] \times C_j \times RC_{ji} \times MIR_j \quad (4)$$

Where, $OFP(i)$ represents the ozone formation potential for a factor number (i) Expressed in µg/m^3. $[VOC_j]$ represents the mixing ratio (ppbv) of a given VOC ion (j), C_j is the number of carbon atoms present in each VOC ion (j), RC_{ji} is the relative contribution of VOC ion (j) to the factor (i). MIR_j is the maximum incremental reactivity of a *VOC* ion (j). The MIR_j are adopted from the (Carter, 2010, 2008, 1994). The above equation is used to compute the OFP for each factor and determine which source factor contributes the most to ozone generation, as explained later. The MIR values are available for a limited number of VOCs, given in supplementary Table S2. The VOCs without reported MIR values are not considered for OFP estimation.

The chemical pathways and reaction products involved in SOA formation from NMVOCs are poorly understood or even unknown. Estimation of SOA formation (SOA yield) has been largely constrained to indirect methods due to the complexity of the chemical matrix of organic aerosols and the lack of direct chemical analysis methods. Numerous studies have estimated SOA yield from different species involving computer modelling and chamber experiments (Zhang et al., 2017). The smog-chamber studies help estimate the value for SOA yield is more reliable as they mimic the actual scenarios. These parameters also helped in improving model parameterisation and SOA mitigation strategies. For the current study, the contribution of an individual NMVOCs species to SOA is estimated by multiplying the SOA yield by the concentration of the NMVOC species in the atmosphere (amount available for the reaction) as shown in Equation. The literature determines the SOA yield (Bruns et al., 2016). The compounds for which SOA yield values are not available from the literature directly, it is estimated that compounds having carbon atoms more than 6 (C >6) will have the same SOA yield of 0.32. The individual SOA yield considered is given in the supplementary Table S3. The contribution of the individual factor to SOA formation is also estimated using (Eq. 5 and 6) as given here.

$$C_{SOA}(j) = Y_{SOA(j)} \times VOC_j \quad (5)$$

$$C_{SOA}(i) = \sum_{j=0}^{n} VOC_j \times RC_{ji} \times Y_{SOA\,(j)} \quad (6)$$

Where, $C_{SOA}(i)$ represents the contribution to SOA formation for a factor number (i) Expressed in µg/m^3. VOC_j represents the concentration (µg/m^3) of a given VOC ion (j), RC_{ji} is the relative contribution of VOC ion (j) to the factor (i). $Y_{SOA\,(j)}$ is the SOA yield of a *VOC* ion (j). The $Y_{SOA\,(j)}$ are adopted from (Bruns et al., 2016).

2.6. CWT back trajectory

Backward trajectory (BT) analysis determines the originating source and transport of air parcels at the receptor location within a specific period. The HYSPLIT model (v4.1 Hybrid Single Particle Lagrangian Integrated Trajectory) was used to perform the BT analysis (Draxler et al., 2018; Stein et al., 2015). The 72-hour back trajectories with a 3-hour time interval at 100 m of arrival height above the ground were calculated using monthly GDAS (Global Data Assimilation System) files (ftp:/arlf tp.arlhq.noaa.gov/pub/archives/gdas1) with a 1◦ × 1◦ resolution. The trajectories were calculated at 100 meters above ground level (AGL). To locate air masses based on their concentrations, the estimated BTs were weighted with VOCs factors time series and averaged over 3-h

https://doi.org/10.5194/egusphere-2022-1165
Preprint. Discussion started: 14 November 2022

intervals using a concentration weight trajectory (CWT) model. ZeFir (Petit et al., 2017), an IGOR-based interface, was used to construct the CWT graphs, as shown in supplementary Figure S3.

3. Results and Discussions

3.1. NMVOCs concentration and temporal variation

The average daily concentrations of measured NMVOCs during the study period is 125.5 ± 37.5 ppbv.Figure 2 shows the daily time series and monthly mean concentrations of NMVOCs, inorganics and organics fractions of Nr-$PM_{2.5}$, O_3, NOx, SO_2, temperature, relative humidity, wind speed, and wind direction. Out of 173 detected ions of NMVOCs, the level of three major species (acetaldehyde, acetone, and acetic acid) are present 5-15 times higher than for other species, as shown in supplementary Figure S2. The monthly averaged concentrations of NMVOCs were observed to decrease from December (193.7 ppbv) to January (110.2 ppbv) till March (101.2 ppbv) and increased sharply during the summer months, April (137.8 ppbv) and May (150.8 ppbv). The highest concentrations of NMVOCs, Nr-$PM_{2.5}$ (inorganics and organics), during the winter months, infer their common sources. In contrast, during the summer months, $PM_{2.5}$ decreases drastically, but NMVOC concentrations are relatively highest, implying additional sources of NMVOCs. High temperatures during warmer periods may lead to more photooxidation of primary VOCs (Sahu et al., 2017), production of biogenic VOCs (Baudic et al., 2016; Sahu et al., 2017) and evaporation of volatile household products (Qin et al., 2021). A difference in temperature conditions during winters (colder) and summers (warmer) leads to more partitioning of the gas phase during summers relatively to winters.

All three abundant NMVOCs present at m/z 45.034 (C_2H_5O, acetaldehyde), 59.049 (C_3H_7O, acetone), and 61.028 ($C_2H_5O_2$, acetic acid) are oxygenated VOCs (OVOCs). The sources of these OVOCs could be direct emissions from biogenic and anthropogenic activities and from the secondary/ photochemical processes also. Diurnal variations of secondary formation, anthropogenic emission level, weather, and PBL heights can be explained by OVOCs/benzene ratios (Sahu et al., 2017, 2016; Tripathi et al., 2022) to some extent. The diurnal patterns of acetaldehyde/benzene, acetone/benzene, and acetic acid/benzene ratios are plotted to check the influence of biogenic and secondary sources (see Figure 3 (a-c)). All the OVOCs/Benzene ratios are observed to increase during the daytime (10-18 h), similar to temperature variation. This infers the influence of photochemical formation and/or biogenic emissions of these compounds. The elevated OVOCs concentrations during the night confirm the influence of anthropogenic emissions.

Acetone and acetaldehyde are formed during photooxidation and ozonolysis of various terpenes and aromatics compounds emitted from multiple biogenic and anthropogenic sources (Lee et al., 2006a, 2006b; S. Wang et al., 2020). Acetone plays a major role in Ozone production. It can be transported to remote areas due to its long lifetime in the troposphere (~15 days) (Seco et al., 2007). The average concentrations of acetone during winters, late winters and summer were observed as 13.6 ±4.5 ppbv, 15.3 ±5.4 ppbv and 34.9 ±10.3 ppbv, respectively. The observed concentrations of acetone in Lucknow are on the higher side of the range of measured concentrations in other Indian cities. The reported average concentrations of acetone in the present study are comparable to Delhi (whole year) is ~16.7 ppbv (13-15 ppbv during winters) (Jain et al., 2022) but higher than Ahmedabad at 5.35 ±1 ppbv during late winters (Sahu et al., 2016), and Mohali as 5.9 ±3.7 ppbv during summers(Sinha et al., 2014). This shows the presence of more OVOCs in cities within the IGB region than in other cities of India.

As shown in Figures 3 (a) and 3 (b), the diurnal variation of acetaldehyde and acetone, respectively, starts increasing from 9 h in the morning to 16h in the evening. The acetaldehyde and acetone had their morning maxima at around 10:00 LT and 11:00 LT, respectively, and later during the morning rush hours of vehicular emissions (8-10h). This trend is similar to a previous study in Ahmedabad (Sahu and Saxena, 2015). It indicates the secondary formation of acetone and acetaldehyde from terpenes and aromatics emitted from vehicles. The OH reaction rate constant of the hydroxyl radical with acetaldehyde (15×10^{-12} cm^3 $molecule^{-1}$ s^{-1}) is significantly higher than the reaction rate constant of the hydroxyl radical with acetone (0.17×10^{-12} cm^3 $molecule^{-1}$ s^{-1}), indicating faster degradation of acetaldehyde than acetone (Atkinson and Arey, 2003).

Figure 3 (c) shows the diurnal variation of acetic acid and acetic acid/ benzene ratio. Acetic acid is one of the most abundant VOC species in the atmosphere globally, having a half-life of more than one day. It contributes to atmospheric acidity (Chebbi and Charlie, 1996) and is responsible for 30% acidity of the wet deposition in polluted urban areas (Seco et al., 2007, Pena et al., 2002). This compound also has toxic effects on human health. Residential wood combustion is one of the critical sources of acetic acid (Bruns et al., 2017). High

https://doi.org/10.5194/egusphere-2022-1165
Preprint. Discussion started: 14 November 2022

levels of acetic acid have also been reported from aged open biomass (hay and straw) burning plumes (Brilli et al., 2014), a variety of biomass fuel (Stockwell et al., 2015), and natural gas (Gilman et al., 2013). The average concentration of acetic acid during the whole study period is about 10.3 ±4.1 ppbv, highest during winters at 15.2 ±3.5 ppbv and lower during summers at 6.9 ±2.1 ppbv. The observed increased concentrations of acetic acid in the winter and lower concentration in the summer may demonstrate its production influenced by open biomass burning crops in nearby fields and residential wood combustion for heating and cooking purposes in Lucknow. The diurnal pattern of acetic acid concentrations shows high concentrations during the night, which infers its accumulation.

3.2. PMF results

This section includes a discussion of the selection of the source apportionment solution and its interpretation. The VOCs factors are identified based on their mass spectra, diurnal and temporal variation, and correlation with external tracers. For the first time, we have included mass spectra of 170 VOC ions from m/z 42. 034 to m/z 197.216 in the PMF analysis. These ions belong to different families based on their chemical composition. They are categorised as aromatics (Ar_CxHy), simple non-aromatics (N_CxHy), furans (Furans), phenols (Phenols), oxygenates: first (CHO_1), second (CHO_2), and third order (CHO_3), nitrogen-containing compounds (CxHyNz and CxHyNzOn) and others. The others include high-order oxygenates (CHO_4) and some hydrocarbons (CxHy). The degree of unsaturation (i.e. the number of rings and/or double bonds) of more than 4 distinguishes aromatic CxHy (Ph CxHy) from the CxHy family. This allowed us to identify important VOCs markers, their families and their role in their atmospheric chemistry.

3.2.1. Optimum solution selection

Unlike the chemical mass balance (CMB) receptor model, the PMF algorithm itself calculates factor profiles. The most crucial decision for the interpretation of the findings of the PMF is selecting the optimum modelled number of factor solutions. This is achieved by applying several mathematical metrics, correlating with external measurements, and interpreting the physical sources. The ratio of Q/Q_{exp} is first examined for every factor solution. The factor solution having an absolute value of Q/ Q_{exp} ratio near 1 indicates an accurate estimation of errors, and it should be selected but not observed for real observations. The $Q/ Q_{exp} >> 1$ and $<< 1$ indicate under and overestimation of errors or variability in the factor solution, respectively. It is anticipated that Q will drop with each addition of the number of factors, as this introduces extra degrees of freedom to improve the fit of the data. Another important metric is the evaluation of scaled residuals over timeseries and mass spectra. The scaled residuals ±3 for each data point in the time series are considered. The supplementary Figure S4 shows the scaled residuals over the timeseries for the 3-7 factor solution. In the present study, the Q/ Q_{exp} does not lie near 1, but the high % change in Q/ Q_{exp} is observed while examining 3-5 factor solutions, as shown in Figure 4. The total scaled residual of all species are calculated and plotted for different number of factors in Figure 4. The changes in the residuals and the drops in Q/Qexp indicate that the 5-factor solution is an optimum solution. Below, this solution is further analysed regarding their mass spectral features, time series and correlation with external tracers.

For further assurance of our chosen solution, the whole dataset was divided into three periods; winter (December), late winter (Jan-march) and summer (April-may). The unconstrained PMF was performed on each period for 2-12 factors and analysed further. The SVOC factor from the unconstrained solution during the late winter period was used to constrain the same factor for the whole period. The constrained profile of SVOC was used for self-constraining with random values varying from 0.1-1 with delta a= 0.1. Finally, a = 0.3 was chosen as the optimum solution after examining the temporal and diurnal variation of the factor. The SVOC factor's constraining helped improve the diurnal variation, which enhanced the confidence in the selected solution.

The uncertainty of the selected solution is quantitatively addressed by bootstrap analysis (Davison and Hinkley, 1997; Paatero et al., 2014), a module available in the SoFi Pro (Canonaco et al., 2021). Previous studies have also followed this methodology for uncertainty estimation of organic aerosols source apportionment (SA) results (Lalchandani et al., 2021; Tobler et al., 2020), elemental aerosols SA results, and VOCs SA results (Wang et al., 2021). This assessment involves randomly resampling the original input data and generating new input data matrices for each run. The variation within the identified factors across all bootstrapped runs allows for estimating the statistical uncertainty if enough resamples been conducted. For the study, the number of resamples is kept at n=500 iterations to check the robustness of the 5-factor solution. Each factor's base case time series was fed into the model to check the variance with each bootstrapped run. Then, based on pre-defined criteria for individual factors, it is observed that 476 out of 500 runs were accepted with a correlation coefficient above 0.9 and a p-

https://doi.org/10.5194/egusphere-2022-1165
Preprint. Discussion started: 14 November 2022

value lower than 0.05. The reported individual mass estimation error for PMF analysis PMF_{error}, for individual factors (i) is calculated by the linear fit method using equation given below (Eq. 7),

$$PMF_{error}, i = 100 \times (\frac{spread}{mean}) \quad (7)$$

Where the spread may refer to the standard deviation and the mean is the averaged concentration of the factor. A linear fit's slope indicates relative inaccuracy when comparing the spread to the mean value. The uncertainty or PMF_{error} is observed as 1% or less for all factors Supplementary Figure S5). This infers that the 5-factor solution is a statistically robust solution with rather low uncertainty.

3.2.2. Profile and diurnal variation

The selected 5-factor PMF solution exhibits distinct mass spectral characteristics related to different sources and atmospheric processes. Figure 5 shows the intricate plots of the profile and diurnal variation of the 5-factor solution. The five factors are Traffic, SFC 1 (Solid Fuel Combustion), SVOC (Secondary volatile organic compounds), SFC 2, and Industrial after thoroughly investigating markers, chemical species and their families, diurnal variation, and relation to meteorological parameters and external measurements. The first factor is identified as traffic. It is characterized by the presence of aromatics, such as benzene (m/z 79.053, C_6H_6H+), toluene (m/z 93.07, C_7H_8H+), xylene (107.09, $C_8H_{10}H+$), C9-aromatics (121.1, $C_9H_{10}H+$), and C10-aromatics (135.12, $C_{10}H_{14}H+$). The diurnal variation shows peaks during rush hours in the morning and evening. The traffic factor in previous studies observed similar markers in Delhi (Jain et al., 2022; Wang et al., 2020) and Beijing (Wang et al., 2021b). Other source-specific studies also identified similar markers for vehicular emissions (Cao et al., 2016; Caplain et al., 2006). The dominant markers in its mass spectra belong to the family of aromatics (~56%), as shown in Figure 6. The CWT graph, as shown in Supplementary Figure S3, shows the probable sources of traffic present near the sampling site.

Another factor which is resolved is Solid Fuel Combustion (SFC 1), have the highest contribution from furans and substituted furans (~36%) and nitrogen-containing compounds (34%), as shown in Figure 5. Furans and nitrogen-containing compounds are mostly emitted from combustion processes (Coggon et al., 2019), cooking fires, burning of peat, crop residue and biomass fuel such as wood, grasses etc. (Stockwell et al., 2015). Studies have also shown that furans and nitrogen-containing compounds have a high potential to form secondary organic aerosols and particles. The prominent signals of acrylonitrile (m/z 54.034, C_3H_4N), furan (m/z 69.033, C_4H_5O), pyridine (80.054, C_5H_6N) furfurals 81.036, C_5H_5O), furaldehyde (m/z 97.027, $C_5H_5O_2$), dimethyl furan (97.064, C_6H_9O), and $C_3H_3N_2O_3$ (115.012) also contribute to the factor's mass spectra as shown in Figure 7 (a). This factor profile is characterised by the strong peak of acetonitrile (m/z 42.034, C_2H_4N) with an explained variation of about ~0.49, as shown in Figure 7 (b). Acetonitrile is considered a unique marker of biomass burning (Holzinger et al., 1999). Other The nitrophenol (m/z 140.033, $C_6H_6NO_3$) and methoxy nitrophenol (m/z 154.054, $C_7H_8NO_3$) is explained by SFC 1 factor profile of ~0.53 and 0.52, respectively. It is reported that phenols in a biomass smoke plume react with NOx to form nitrophenol, considered a unique marker for aged biomass burning smoke (Harrison et al., 2005; Mohr et al., 2013). Nitrophenols and other nitrogen-containing aerosols act as cloud condensation nuclei (Kerminen et al., 2005; Laaksonen et al., 2005; Sotiropoulou et al., 2006), and contribute to the formation of SOA and light-absorbing brown carbon aerosols (Laskin et al., 2009; Mohr et al., 2013). This factor may belong to the aged biomass-burning plume, transported from sources located on the outskirts of the city and nearby districts. The city is surrounded by various agricultural fields, which generally involve open biomass burning activities. The back trajectory analysis of the factor also shows the probable sources in nearby areas, mainly coming from the west direction of the sampling site (supplementary Figure S3).

The third factor, Solid Fuel Combustion (SFC 2), was identified in the 5-factor solution. The unique characteristic of this factor is its presence only in December. Lower ambient temperature and high relative humidity during this month are responsible for the different chemical pathways for the fate of compounds. The factor profile explains 53% of phenols. 23% of second-order oxygenates, 30% of furans and 21% of nitrogen-containing compounds are also present in the factor profile. Commonly used domestic fuels other than liquid petroleum gas (LPG) in the Indian sub-continent are cow dung, fuelwood, and peat, in different proportions depending upon their composition and availability. A previous study (Stewart et al., 2021b) observed phenols are released from the combustion of fuelwood (22-80%), followed by crop residue (32-57%), cow dung cake (32-36%), and municipal solid waste (24-37%). The combustion process at a higher temperature leads to the

https://doi.org/10.5194/egusphere-2022-1165
Preprint. Discussion started: 14 November 2022

depolymerisation of lignin content in the biomass, which allows the aromatisation process to give off phenols, substituted phenolic compounds, and non-substituted aromatics (Sekimoto et al., 2018; Simoneit et al., 1993). The lower ambient temperature during December is responsible for increased burning activities for cooking and heating purposes. The factor's mass spectra is characterized with peak signals of methyl furan (m/z 83.049, C_5H_7O), phenol (m/z 95.049, C_6H_7O), cresol (m/z 109.06, C_7H_9O), catechol (m/z 111.043, $C_6H_7O_2$), phenyl butanedione (m/z 163.115, $C_{10}H_{11}O_2$), hexene (m/z 85.093, C_6H_{13}), as shown in Figure 5 (a). The SFC 1 and SFC 2 factor profile is compared with each other in Figure 7 (a). It explains the similar NMVOCs are present in the factors, but the intensity of the signal is different. This is due to the difference in the emission sources and chemical pathways of formation. For example, High molecular weighted and more substituted phenolic compounds such as guaiacol (m/z 125.059, $C_7H_9O_2$) and cresol are released at the early stages of the smouldering stage of the fire (lower temperature), and low molecular weighted phenols are released during later stages (high temperature) (Stewart et al., 2021a). The higher explained variation from cresol (~0.8) and guaiacol (0.21) to the factor's profile indicate their new emissions from residential heating activities and the burning of sawdust (Stewart et al., 2021a), as shown in Figure 7 (b). Other compounds like phenols (0.27) and hexene (~0.62) are explained by this SFC 2 factor's profile. These two compounds are being reported in the emissions from local biomass burning of wood in an Indian city (Delhi)(Stewart et al., 2021).

The fourth factor, secondary volatile organic compounds (SVOC), has the highest contribution from second-order oxygenates (40 %) and third-order oxygenates (40%), as shown in Figure 6. The relative composition of the profile of the factor reveals significant signals of acetic acid (m/z 77.019, $C_2H_5O_3$), propylene glycol (m/z 77.048, $C_3H_9O_2$), methylglyoxal (m/z 73.028, $C_3H_5O_2$), methyl methacrylate (93.033 C_6H_5O), and $C_5H_9O_2$ (m/z 101.059). Lower contributions from first-order oxygenate than the second, and third-order oxygenates indicate that these OVOCs are products of various photochemical and oxidation processes in the atmosphere instead of their direct emissions. The diurnal mean concentration of the SVOC factor in Figure 5 (b) shows distinct day-to-night variation, following the pattern of solar radiation. The mean concentration increases during the morning (8:00), peaks during the afternoon hours (12:00-15:00), and decreases towards the evening (20:00). The nighttime concentration of the factor is lowest due to the absence of photochemical activity at night. Small organic acids like formic acid (m/z 47.012, CH_3O_2) could potentially come from the photooxidation of furans and aromatics (Stewart et al., 2021a; Wang et al., 2020), which contribute 42.2% to the SVOC factor's profile (Figure 6). Other compounds like methoxyphenols are released by biomass burning, which is further photo-oxidised, resulting in the formation of SOA (Li et al., 2014; Yee et al., 2013). Figure 7 (b) shows the explained variation of these compounds, such as vanillin (methoxyphenol) and syringol (2,6-dimethoxyphenol) to the SVOC factor is ~0.57 and 0.41, respectively, relatively high. This also confirms the association of products and intermediate products of photochemical reactions with the SVOC factor.

The Volatile Chemical products (VCPs) factor is identified with prominent signals of formaldehyde (m/z 31.018, CH_3O), ethanol (m/z 47.049, C_2H_6O), naphthalene (m/z 129.05, $C_{10}H_9$). Formaldehyde and ethanol are used as solvents in the paint, solvent-based, textile, plastics, and automobile industries. Formaldehyde is also commonly used as an industrial disinfectant, fungicide, and germicide. 62.4% and 76.6% of the formaldehyde and ethanol contribute to the industrial factor. Many solvent-based and textile industries are present in the close vicinity of the sampling site, which is possibly the reason for the high concentration of formaldehyde and ethanol. Shorter-life spans of formaldehyde (~1 hour) and ethanol (~3-4 hours) in the atmosphere confirms their emissions from local source instead of transport from regional sources. The relative contribution of naphthalene is about 28.3%, respectively, to the factor. Other dominant signals of naphthalene diamine (m/z 159.102, $C_{10}H_{11}N_2$) and methoxy benzopyranone (m/z 177.056, $C_{10}H_9O_3$) relatively contribute about 34.5% and 44.45% to the factor. Naphthalene is present in ambient air due to emissions from the industries such as primary metal industries, chemical manufacturing industries, and pharmaceuticals (Preuss et al., 2003). Naphthalene is also used as an intermediate product in coal tar, dyes or inks, leather tanning and asphalt industries (Jia and Batterman, 2010). It is classified as a possible human carcinogen and precursor of atmospheric SOA (Jia and Batterman, 2010; Tang et al., 2020).

It is observed that there are very sharp peaks in the concentrations of formaldehyde, ethanol, naphthalene, naphthalene diamine and benzopyrene in the high-resolution timeseries, as shown in supplementary Figure S6. This may be due to the influence of particular activity in near-by industries. A conglomerate of the industries is present in the southwest direction of the sampling site within and outside the city, as shown in Figure 1. The direction of the wind changes to the southwest during summers may have brought the high levels of naphthalene and its derivatives emitted from these industrial areas to the sampling site. The CWT graph also shows the strong

https://doi.org/10.5194/egusphere-2022-1165
Preprint. Discussion started: 14 November 2022

influence of the source present in the southwest direction of the sampling site (supplementary Figure S3). A previous study has found that among the emitted OVOCs from sewage sludge, first-order OVOCs constituent ~60%, followed by high-order OVOCs (Haider et al., 2022).

Interestingly, there are three sewage treatment plants located near the sampling site. They may have influenced the concentrations of OVOCs at the sampling site. The influence of factor contribution during summertime is probably due to the increased production of naphthalene, formaldehyde, and ethanol from their local industrial sources and secondary formations at higher temperatures, as shown in the time series of the factors (supplementary Figure S7).

3.3. Correlation with AMS factors and other external factors

The timeseries of the five factors resolved from NMVOCs mass spectra are co-related with external measurements such as oxygenated organic aerosols (OOA), Black carbon (BC) concentrations, CAAQMS data (WD, WS, RH, Temp, NO, NO2, NOX, SO2, Ozone) as given in Figure 8. The VOC's traffic factor shows a temporal correlation (Pearson r^2 ~ 0.43) with nitrogen oxides (NO_X), which is also an indicator of vehicular emissions. This infers the NOx emissions along with NMVOCs from the vehicular fleet. Similarly, SFC 1 factor correlates with organics fraction of Nr- PM2.5 (Org_Hr), NO_3_Hr (inorganics NO3 of Nr- $PM_{2.5}$) and RH well with Pearson r^2 ~ 0.46, 0.53, and 0.47, respectively. The correlation coefficient between SFC 2 and black carbon concentrations is ~0.4. Volatile chemical products show good temporal co-relation with a solvent-based NMVOCs species, acetone, with Pearson r^2 ~ 0.6.

Figure 9 shows the scatter plots of individual VOC factors correlated with the most probable related sources, resolved after performing the PMF analysis on the mass spectra of the organic portion of NR- $PM_{2.5}$ (non-refractory $PM_{2.5}$) measured by HR-ToF-AMS during the campaign. The detailed analysis and results of PMF of NR- $PM_{2.5}$ are given in other studies (Lalchandani et al., 2021; Talukdar et al., 2021; Tobler et al., 2020), beyond the scope of this paper. In brief, the organic aerosols (OA) mass spectra from HR-ToF-AMS were explained by 5-factors consisting of one hydrocarbon-like organic aerosols factor (AMS_HOA), two solid fuel combustion factors (AMS_SFC/BB& AMS_SFC/OA), one more-oxidised oxygenated OA (AMS_MO-OOA) and one low-oxidised oxygenated OA (AMS_LO-OOA). In this study, the traffic factor resolved from VOCs mass spectra has a good correlation (Pearson r^2 ~ 0.65) with the AMS_HOA, as shown in Figure 9 (a). This AMS_HOA factor is characterised by aliphatic hydrocarbons, typically associated with traffic exhaust emissions (Lalchandani et al., 2021). It infers that vehicular exhaust is one of the common sources influencing the release of VOCs and primary OA. These VOCs and primary OA also exhibit similar diurnal solid variation, having sharp peaks during morning and evening hours during the rush hours, as shown in supplementary Figure S7.

The SFC factors resolved from organic mass spectra contained significant signals from unsaturated hydrocarbons, polyaromatic hydrocarbons, and oxygenated fragments ((Lalchandani et al., 2021; Shukla et al., 2021). The AMS_SFC/OA factor relates to the primary emissions from the combustion process of wood and paper, and biomass is influenced by a higher O/C (~0.878) ratio than the AMS_SFC/BB O/C ratio (~0.268). The resolved factor from VOCs mass spectra related to biomass burning (SFC 1) shows a strong temporal correlation (Pearson r2 ~ 0.85) with AMS_SFC/OA. Thus, we interpret SFC 1 as more related to conventional biomass burning at the site. The correlation of SFC 1 with organics Nr-PM2.5 This argues that the domestic usage of biomass for cooking and other purposes is one of the leading factors for primary emissions of gas-phase (SFC 1) and particle-phase oxygenates (OOA). The factor SFC 2, derived from the VOC mass spectra, is more related (Pearson r^2 ~0.54) to the AMS_MO-OOA as shown in Figure 9 (c) and supplementary Figure S7. AMS_MO-OOA is characterised by higher m/z 44 (CO_2) and m/z 43 (C_2H_3O) fractions than the primary OA sources. This factor is comparatively more oxidised, having an O/C ratio of ~0.89 than AMS_LO-OOA (O/C ratio ~0.62). We interpret that SFC 2 is influenced by fresh oxidation of primary biomass burning emissions.

3.4. OFP and SOA yield from individual sources

Based on the method explained in section 2.5, the ozone formation potential was calculated for each factor after considering the MIR values of VOCs ions as given in supplementary Table S2. The relative contribution of each VOCs ions to the individual factor after PMF analysis is multiplied by the averaged individual concentration of the VOC ion. The highest contributor species to the ozone formation potential is toluene, followed by xylene, isoprene, and formaldehyde. The distribution of individual sources to OFP is shown in Figure 10 (a). The traffic factor contributes maximum to the OFP among all the factors with 34.6%, followed by SFC1 (23.9%), then SFC 2(14.5%), SVOC (13.5%) and VCPs (13.5%).

https://doi.org/10.5194/egusphere-2022-1165
Preprint. Discussion started: 14 November 2022

Similarly, the contribution towards the formation of SOA is also estimated for each factor with SOA yield of individual VOCs ions as given in supplementary Table S3. The overall SOA yield is influenced by toluene, benzene, phenol, methyl furan, naphthalene, xylene, and trimethyl benzene. These compounds mostly belong to the aromatics family. This shows the role of aromatic VOC species in the formation of SOA. The primary factors, Traffic and SFC 1, are the highest contributors to the SOA formation at 28% and 27%, respectively, as shown in Figure 10 (b). These factors are ridden with the highest SOA formation contributing VOCs species. The SVOC factor contributes 22% to the SOA formation, with maximum contribution from high-molecular oxygenated species. The SFC 2 and VCPs are less contributing towards the SOA formation.

In contrast, this sequence is not similar to the relative contribution of the sources according to their concentration (Figure 10 (c)). The source contributing to the highest concentration of NMVOCs is SFC 1, followed by traffic, SVOC, and VCPs. The lowest contributor is SFC 2. This comparison shows the importance of the source of NMVOCs towards SOA and ozone chemistry. The factor contributing the highest to the concentration of NMVOCs may not necessarily influence the ozone and SOA formation in the same way. This method merely represents the complex behaviour of NMVOCs, NOx and solar radiation for producing tropospheric ozone and SOA. There are many NMVOCs species with unknown ozone and SOA yield values. More research on the section is needed.

4. Conclusion

This study investigated the high time-resolved chemical characterisation of NMVOCs in Lucknow between December 2020 and May 2021. The mass spectra are used to perform source apportionment and study the diurnal variations. The individual species are identified as per their chemical formula and exhibit large temporal fluctuations. The highest NMVOCs concentrations during winters are due to their increased emissions from solid fuel combustion and stagnant conditions due to less mixing height. The warmer period between April and May shows the influence of high photochemical activity and regional transport. The major industries lie in the southwest direction of the sampling site, which may be responsible for elevated volatile chemical products during summer. The five major factors resolved from source apportionment are a traffic factor, two solid fuel combustion factors, secondary VOCs, and VCPs. The primary sources, such as traffic factor and solid fuel combustion, exhibit a stronger correlation with organic aerosol resolved factors, infers their common time of origin from similar sources. The traffic factor has a similar profile found in Delhi, which infers a similar vehicular pattern and fuel composition in different urban centres of the IGB region of India. The biomass burning factors have distinct profiles from Delhi due to different cooking or domestic fuel consumption and cropping patterns. The VCPs factor significantly contributes to primary first-order oxygenates, while the secondary VOCs factor has second and third-order oxygenates. The highest contributing factor in Lucknow was found as solid fuel combustion and traffic. The NMVOCs and NOx derive from the formation of ozone and SOA, but there is limited knowledge of their complex relationship. However, ozone and SOA formations are estimated using available studies in the best way possible. There is a scope for improving these values in further studies. It is interesting to note that the primary factors, Traffic and SFC 1, are crucial in Lucknow city for NMVOCs emissions and ozone and SOA formation. These sources are highly influenced by local emissions, meteorology, city planning and implementation of the policies. Further studies focusing on VOCs-secondary organic aerosol interactions would help identify the gas-particle partitioning, ageing and transport of pollution in the region.

5. Data availability

The data is available on the request with corresponding author.

6. Author Contribution

Vaishali Jain: Conceptualization, data curation, Methodology, Software, Validation, Formal analysis, Investigation, Writing– original draft, Writing– review & editing, Visualization **Sachchida N. Tripathi:** Conceptualization, Writing– review & editing, Supervision, Project administration, Funding acquisition **Nidhi Tripathi:** Investigation, Data curation, Validation, Writing– review & editing, **Mansi Gupta:** Investigation, Data curation, Validation, Writing– review & editing, **Lokesh K. Sahu:** Resources, Methodology, Validation, Writing– review & editing **Sreenivas Gaddamidi:** Investigation, Data curation, Validation, **Ashutosh K. Shukla:** Validation, Writing– review & editing, **Vishnu Murari:** Formal analysis, Validation, Writing– review & editing, **Andre S.H. Prevot:** Methodology, Validation, Writing– review & editing.

https://doi.org/10.5194/egusphere-2022-1165
Preprint. Discussion started: 14 November 2022

7. Competing interests

The authors declare that they have no known competing financial interests or personal relationships that could have appeared to influence the work reported in this paper.

8. Acknowledgements

LKS, NT and MG acknowledge Prof. Anil Bhardwaj, Director, Physical Research Laboratory (PRL), Ahmedabad, India, for the support and permission to deploy PTR-TOF-MS during the experimental campaign. SNT and VJ gratefully acknowledge the financial support provided from Swiss Agency for Development and Cooperation, Switzerland to conduct this research under project no. 7F-10093. 01. 04 (contract no. 81062452). SNT also acknowledges the support from Duke University, Office of Research Support, Subaward no. 349-0685.

9. References

Atkinson, R., Arey, J., 2003. Atmospheric Degradation of Volatile Organic Compounds. Chem. Rev. 103, 4605–4638. https://doi.org/10.1021/cr0206420

Balakrishnan, K., Chen, G., Brauer, M., Chow, J., 2015. IARC Monographs on the Evaluation of Carcinogenic Risks to Humans: Outdoor Air Pollution, IARC , WHO.

Baudic, A., Gros, V., Sauvage, S., Locoge, N., Sanchez, O., Sarda-Estève, R., Kalogridis, C., Petit, J.E., Bonnaire, N., Baisnée, D., Favez, O., Albinet, A., Sciare, J., Bonsang, B., 2016. Seasonal variability and source apportionment of volatile organic compounds (VOCs) in the Paris megacity (France). Atmos. Chem. Phys. 16, 11961–11989. https://doi.org/10.5194/acp-16-11961-2016

Blake, R.S., Monks, P.S., Ellis, A.M., 2009. Proton-transfer reaction mass spectrometry. Chem. Rev. 109, 861–896. https://doi.org/10.1021/cr800364q

Blake, R.S., Whyte, C., Hughes, C.O., Ellis, A.M., Monks, P.S., 2004. Demonstration of proton-transfer reaction time-of-flight mass spectrometry for real-time analysis of trace volatile organic compounds. Anal. Chem. 76, 3841–3845. https://doi.org/10.1021/ac0498260

Brief Industrial Profile of District Lucknow, Uttar Pradesh, 2018. . Lucknow.

Brilli, F., Gioli, B., Ciccioli, P., Zona, D., Loreto, F., Janssens, I.A., Ceulemans, R., 2014. Proton Transfer Reaction Time-of-Flight Mass Spectrometric (PTR-TOF-MS) determination of volatile organic compounds (VOCs) emitted from a biomass fire developed under stable nocturnal conditions. Atmos. Environ. 97, 54–67. https://doi.org/10.1016/j.atmosenv.2014.08.007

Bruns, E.A., El Haddad, I., Slowik, J.G., Kilic, D., Klein, F., Baltensperger, U., Prévôt, A.S.H., 2016. Identification of significant precursor gases of secondary organic aerosols from residential wood combustion. Sci. Rep. 6, 1–9. https://doi.org/10.1038/srep27881

Bruns, E.A., Slowik, J.G., El Haddad, I., Kilic, D., Klein, F., Dommen, J., Temime-Roussel, B., Marchand, N., Baltensperger, U., Prévôt, A.S.H., 2017. Characterization of gas-phase organics using proton transfer reaction time-of-flight mass spectrometry: Fresh and aged residential wood combustion emissions. Atmos. Chem. Phys. 17, 705–720. https://doi.org/10.5194/acp-17-705-2017

Canonaco, F., Crippa, M., Slowik, J.G., Baltensperger, U., Prévôt, A.S.H., 2013. SoFi, an IGOR-based interface for the efficient use of the generalized multilinear engine (ME-2) for the source apportionment: ME-2 application to aerosol mass spectrometer data. Atmos. Meas. Tech. 6, 3649–3661. https://doi.org/10.5194/amt-6-3649-2013

Canonaco, F., Tobler, A., Chen, G., Sosedova, Y., Gates Slowik, J., Bozzetti, C., Rudolf Daellenbach, K., El Haddad, I., Crippa, M., Huang, R.J., Furger, M., Baltensperger, U., Prévôt, A.S.H., 2021. A new method for long-term source apportionment with time-dependent factor profiles and uncertainty assessment using SoFi Pro: Application to 1 year of organic aerosol data. Atmos. Meas. Tech. 14, 923–943. https://doi.org/10.5194/amt-14-923-2021

Cao, X., Yao, Z., Shen, X., Ye, Y., Jiang, X., 2016. On-road emission characteristics of VOCs from light-duty gasoline vehicles in Beijing, China. Atmos. Environ. 124, 146–155. https://doi.org/10.1016/j.atmosenv.2015.06.019

Caplain, I., Cazier, F., Nouali, H., Mercier, A., Déchaux, J.C., Nollet, V., Joumard, R., André, J.M., Vidon, R., 2006. Emissions of unregulated pollutants from European gasoline and diesel passenger cars. Atmos.

https://doi.org/10.5194/egusphere-2022-1165
Preprint. Discussion started: 14 November 2022

Environ. 40, 5954–5966. https://doi.org/10.1016/j.atmosenv.2005.12.049

Carter, W., 2010. UPDATED MAXIMUM INCREMENTAL REACTIVITY SCALE AND HYDROCARBON BIN REACTIVITIES FOR REGULATORY APPLICATIONS.

Carter, W.P.L., 2008. Reactivity Estimates for Selected consumer product compounds.

Carter, W.P.L., 1994. Development of ozone reactivity scales for volatile organic compounds. J. Air Waste Manag. Assoc. 44, 881–899. https://doi.org/10.1080/1073161x.1994.10467290

Chameides, W.L., Fehsenfeld, F., Rodgers, M.O., Cardelino, C., Martinez, J., Parrish, D., Lonneman, W., Lawson, D.R., Rasmussen, R.A., Zimmerman, P., Greenberg, J., Middleton, P., Wang, T., 1992. Ozone precursor relationships in the ambient atmosphere. J. Geophys. Res. 97, 6037–6055. https://doi.org/10.1029/91JD03014

Coggon, M.M., Lim, C.Y., Koss, A.R., Sekimoto, K., Yuan, B., Gilman, J.B., Hagan, D.H., Selimovic, V., Zarzana, K.J., Brown, S.S., M Roberts, J., Müller, M., Yokelson, R., Wisthaler, A., Krechmer, J.E., Jimenez, J.L., Cappa, C., Kroll, J.H., De Gouw, J., Warneke, C., 2019. OH chemistry of non-methane organic gases (NMOGs) emitted from laboratory and ambient biomass burning smoke: Evaluating the influence of furans and oxygenated aromatics on ozone and secondary NMOG formation. Atmos. Chem. Phys. 19, 14875–14899. https://doi.org/10.5194/acp-19-14875-2019

Davison, A.C., Hinkley, D. V., 1997. Bootstrap Methods and their Application. Cambridge University Press. https://doi.org/10.1017/CBO9780511802843

Decarlo, P.F., Kimmel, J.R., Trimborn, A., Northway, M.J., Jayne, J.T., Aiken, A.C., Gonin, M., Fuhrer, K., Horvath, T., Docherty, K.S., Worsnop, D.R., Jimenez, J.L., 2006. Field-Deployable, High-Resolution, Time-of-Flight Aerosol Mass Spectrometer. Anal. Chem. 78, 8281–8289. https://doi.org/8410.1029/2001JD001213.Analytical

Gilman, J.B., Lerner, B.M., Kuster, W.C., De Gouw, J.A., 2013. Source signature of volatile organic compounds from oil and natural gas operations in northeastern Colorado. Environ. Sci. Technol. 47, 1297–1305. https://doi.org/10.1021/es304119a

Government of India, M. of R.T. and H.T.R. wing, 2019. Road Transport Year Book (2016-17).

Graus, M., Müller, M., Hansel, A., 2010. High resolution PTR-TOF: Quantification and Formula Confirmation of VOC in Real Time. J. Am. Soc. Mass Spectrom. 21, 1037–1044. https://doi.org/10.1016/j.jasms.2010.02.006

Haider, K.M., Lafouge, F., Carpentier, Y., Houot, S., Petitprez, D., Loubet, B., Focsa, C., Ciuraru, R., 2022. Chemical identification and quantification of volatile organic compounds emitted by sewage sludge. Sci. Total Environ. 838. https://doi.org/10.1016/j.scitotenv.2022.155948

Harrison, M.A.J., Barra, S., Borghesi, D., Vione, D., Arsene, C., Iulian Olariu, R., 2005. Nitrated phenols in the atmosphere: A review. Atmos. Environ. 39, 231–248. https://doi.org/10.1016/j.atmosenv.2004.09.044

Holzinger, R., Wameke, C., Hansel, A., Jordan, A., Lindinger, W., Scharffe, D.H., Schade, G., Crutzen, P.J., 1999. Biomass burning as a source of formaldehyde, acetaldehyde, methanol, acetone, acetonitrile, and hydrogen cyanide. Geophys. Res. Lett. 26, 1161–1164. https://doi.org/10.1029/1999GL900156

Jain, V., Tripathi, S.N., Tripathi, N., Sahu, L.K., Gaddamidi, S., Shukla, A.K., Bhattu, D., Ganguly, D., 2022. Seasonal variability and source apportionment of non-methane VOCs using PTR-TOF-MS measurements in Delhi , India. Atmos. Environ. 283, 119163. https://doi.org/10.1016/j.atmosenv.2022.119163

Jia, C., Batterman, S., 2010. A critical review of naphthalene sources and exposures relevant to indoor and outdoor air. Int. J. Environ. Res. Public Health 7, 2903–2939. https://doi.org/10.3390/ijerph7072903

Jordan, A., Haidacher, S., Hanel, G., Hartungen, E., Märk, L., Seehauser, H., Schottkowsky, R., Sulzer, P., Märk, T.D., 2009. A high resolution and high sensitivity proton-transfer-reaction time-of-flight mass spectrometer (PTR-TOF-MS). Int. J. Mass Spectrom. 286, 122–128. https://doi.org/10.1016/j.ijms.2009.07.005

Kerminen, V.M., Lihavainen, H., Komppula, M., Viisanen, Y., Kulmala, M., 2005. Direct observational evidence linking atmospheric aerosol formation and cloud droplet activation. Geophys. Res. Lett. 32, 1–4. https://doi.org/10.1029/2005GL023130

https://doi.org/10.5194/egusphere-2022-1165
Preprint. Discussion started: 14 November 2022

Laaksonen, A., Hamed, A., Joutsensaari, J., Hiltunen, L., Cavalli, F., Junkermann, W., Asmi, A., Fuzzi, S., Facchini, M.C., 2005. Cloud condensation nucleus production from nucleation events at a highly polluted region. Geophys. Res. Lett. 32, 1–4. https://doi.org/10.1029/2004GL022092

Lalchandani, V., Kumar, V., Tobler, A., M. Thamban, N., Mishra, S., Slowik, J.G., Bhattu, D., Rai, P., Satish, R., Ganguly, D., Tiwari, Suresh, Rastogi, N., Tiwari, Shashi, Močnik, G., Prévôt, A.S.H., Tripathi, S.N., 2021. Real-time characterization and source apportionment of fine particulate matter in the Delhi megacity area during late winter. Sci. Total Environ. 770. https://doi.org/10.1016/j.scitotenv.2021.145324

Laskin, A., Smith, J.S., Laskin, J., 2009. Molecular characterization of nitrogen-containing organic compounds in biomass burning aerosols using high-resolution mass spectrometry. Environ. Sci. Technol. 43, 3764–3771. https://doi.org/10.1021/es803456n

Lawrence, A., Fatima, N., 2014. Urban air pollution & its assessment in Lucknow City - The second largest city of North India. Sci. Total Environ. 488–489, 447–455. https://doi.org/10.1016/j.scitotenv.2013.10.106

Lee, A., Goldstein, A.H., Keywood, M.D., Gao, S., Ng, N.L., Varutbangkul, V., Bahreini, R., Flagan, R.C., Seinfeld, J.H., 2006a. Gas-phase products and secondary aerosol yields from the ozonolysis of ten different terpenes. J. Geophys. Res. Atmos. 111. https://doi.org/doi:10.1029/2005JD006437

Lee, A., Goldstein, A.H., Kroll, J.H., Ng, N.L., Varutbangkul, V., Flagan, R.C., Seinfeld, J.H., 2006b. Gas-phase products and secondary aerosol yields from the photooxidation of 16 different terpenes. J. Geophys. Res. Atmos. 111. https://doi.org/doi:10.1029/2006JD007050

Li, Y.J., Huang, D.D., Cheung, H.Y., Lee, A.K.Y., Chan, C.K., 2014. Aqueous-phase photochemical oxidation and direct photolysis of vanillin - A model compound of methoxy phenols from biomass burning. Atmos. Chem. Phys. 14, 2871–2885. https://doi.org/10.5194/acp-14-2871-2014

Markandeya, Verma, P.K., Mishra, V., Singh, N.K., Shukla, S.P., Mohan, D., 2021. Spatio-temporal assessment of ambient air quality, their health effects and improvement during COVID-19 lockdown in one of the most polluted cities of India. Environ. Sci. Pollut. Res. 28, 10536–10551. https://doi.org/10.1007/s11356-020-11248-3

Mohr, C., Lopez-Hilfiker, F.D., Zotter, P., Prévoît, A.S.H., Xu, L., Ng, N.L., Herndon, S.C., Williams, L.R., Franklin, J.P., Zahniser, M.S., Worsnop, D.R., Knighton, W.B., Aiken, A.C., Gorkowski, K.J., Dubey, M.K., Allan, J.D., Thornton, J.A., 2013. Contribution of nitrated phenols to wood burning brown carbon light absorption in detling, united kingdom during winter time. Environ. Sci. Technol. 47, 6316–6324. https://doi.org/10.1021/es400683v

Müller, M., Graus, M., Wisthaler, A., Hansel, A., Metzger, A., Dommen, J., Baltensperger, U., 2012. Analysis of high mass resolution PTR-TOF mass spectra from 1,3,5-trimethylbenzene (TMB) environmental chamber experiments. Atmos. Chem. Phys. 12, 829–843. https://doi.org/10.5194/acp-12-829-2012

Paatero, P., 1999. The Multilinear Engine—A Table-Driven, Least Squares Program for Solving Multilinear Problems, Including the n-Way Parallel Factor Analysis Model. J. Comput. Graph. Stat. 8, 854–888. https://doi.org/10.1080/10618600.1999.10474853

Paatero, P., Eberly, S., Brown, S.G., Norris, G.A., 2014. Methods for estimating uncertainty in factor analytic solutions. Atmos. Meas. Tech. 7, 781–797. https://doi.org/10.5194/amt-7-781-2014

Paatero, P., Hopke, P.K., 2003. Discarding or downweighting high-noise variables in factor analytic models. Anal. Chim. Acta 490, 277–289. https://doi.org/10.1016/S0003-2670(02)01643-4

Paatero, P., Tapper, U., 1994. Positive matrix factorization: A non-negative factor model with optimal utilization of error estimates of data values. Environmetrics 5, 111–126. https://doi.org/10.1002/env.3170050203

Paatero, P., Tapper, U., 1993. Analysis of different modes of factor analysis as least squares fit problems. Chemom. Intell. Lab. Syst. 18, 183–194. https://doi.org/10.1016/0169-7439(93)80055-M

Pandey, P., Khan, A.H., Verma, A.K., Singh, K.A., Mathur, N., Kisku, G.C., Barman, S.C., 2012. Seasonal trends of PM 2.5 and PM 10 in ambient air and their correlation in ambient air of Lucknow City, India. Bull. Environ. Contam. Toxicol. 88, 265–270. https://doi.org/10.1007/s00128-011-0466-x

Pandey, P., Patel, D.K., Khan, A.H., Barman, S.C., Murthy, R.C., Kisku, G.C., 2013. Temporal distribution of fine particulates (PM 2.5, PM 10), potentially toxic metals, PAHs and Metal-bound carcinogenic risk in the

https://doi.org/10.5194/egusphere-2022-1165
Preprint. Discussion started: 14 November 2022

population of Lucknow City, India. J. Environ. Sci. Heal. - Part A Toxic/Hazardous Subst. Environ. Eng. 48, 730–745. https://doi.org/10.1080/10934529.2013.744613

Petit, J.E., Favez, O., Albinet, A., Canonaco, F., 2017. A user-friendly tool for comprehensive evaluation of the geographical origins of atmospheric pollution: Wind and trajectory analyses. Environ. Model. Softw. 88, 183–187. https://doi.org/10.1016/j.envsoft.2016.11.022

Preuss, R., Angerer, J., Drexler, H., 2003. Naphthalene - An environmental and occupational toxicant. Int. Arch. Occup. Environ. Health 76, 556–576. https://doi.org/10.1007/s00420-003-0458-1

Qin, M., Murphy, B.N., Isaacs, K.K., McDonald, B.C., Lu, Q., McKeen, S.A., Koval, L., Robinson, A.L., Efstathiou, C., Allen, C., Pye, H.O.T., 2021. Criteria pollutant impacts of volatile chemical products informed by near-field modelling. Nat. Sustain. 4, 129–137. https://doi.org/10.1038/s41893-020-00614-1

Sahu, L.K., Saxena, P., 2015. High time and mass resolved PTR-TOF-MS measurements of VOCs at an urban site of India during winter: Role of anthropogenic, biomass burning, biogenic and photochemical sources. Atmos. Res. 164–165, 84–94. https://doi.org/10.1016/j.atmosres.2015.04.021

Sahu, L.K., Tripathi, N., Yadav, R., 2017. Contribution of biogenic and photochemical sources to ambient VOCs during winter to summer transition at a semi-arid urban site in India. Environ. Pollut. 229, 595–606. https://doi.org/10.1016/j.envpol.2017.06.091

Sahu, L.K., Yadav, R., Pal, D., 2016. Source identification of VOCs at an urban site of western India: Effect of marathon events and anthropogenic emissions. J. Geophys. Res. Atmos. Res. 121, 2416–2433. https://doi.org/10.1002/2015JD024454

Seco, R., Peñuelas, J., Filella, I., 2007. Short-chain oxygenated VOCs: Emission and uptake by plants and atmospheric sources, sinks, and concentrations. Atmos. Environ. 41, 2477–2499. https://doi.org/10.1016/j.atmosenv.2006.11.029

Sekimoto, K., Koss, A.R., Gilman, J.B., Selimovic, V., Coggon, M.M., Zarzana, K.J., Yuan, B., Lerner, B.M., Brown, S.S., Warneke, C., Yokelson, R.J., Roberts, J.M., De Gouw, J., 2018. High-and low-temperature pyrolysis profiles describe volatile organic compound emissions from western US wildfire fuels. Atmos. Chem. Phys. 18, 9263–9281. https://doi.org/10.5194/acp-18-9263-2018

Sharma, K., Singh, R., Barman, S.C., Mishra, D., Kumar, R., Negi, M.P.S., Mandal, S.K., Kisku, G.C., Khan, A.H., Kidwai, M.M., Bhargava, S.K., 2006. Comparison of trace metals concentration in PM10 of different locations of Lucknow City, India. Bull. Environ. Contam. Toxicol. 77, 419–426. https://doi.org/10.1007/s00128-006-1082-z

Sharma, S., Khare, M., 2017. Simulating ozone concentrations using precursor emission inventories in Delhi – National Capital Region of India. Atmos. Environ. 151, 117–132. https://doi.org/10.1016/j.atmosenv.2016.12.009

Shukla, A.K., Lalchandani, V., Bhattu, D., Dave, J.S., Rai, P., Thamban, N.M., Mishra, S., Gaddamidi, S., Tripathi, N., Vats, P., Rastogi, N., Sahu, L., Ganguly, D., Kumar, M., Singh, V., Gargava, P., Tripathi, S.N., 2021. Real-time quantification and source apportionment of fine particulate matter including organics and elements in Delhi during summertime. Atmos. Environ. 261. https://doi.org/10.1016/j.atmosenv.2021.118598

Simonelt, B.R.T., Rogge, W.F., Mazurek, M.A., Standley, L.J., Hildemann, L.M., Cass, G.R., 1993. Lignin Pyrolysis Products, Lignans, and Resin Acids as Specific Tracers of Plant Classes in Emissions from Biomass Combustion. Environ. Sci. Technol. 27, 2533–2541. https://doi.org/10.1021/es00048a034

Sinha, V., Kumar, V., Sarkar, C., 2014. Chemical composition of pre-monsoon air in the Indo-Gangetic Plain measured using a new air quality facility and PTR-MS: High surface ozone and strong influence of biomass burning. Atmos. Chem. Phys. 14, 5921–5941. https://doi.org/10.5194/acp-14-5921-2014

Smith, D., Spanel, P., 2005. Selected ion flow tube mass spectrometry SIFT-MS for on-line trace gas analysis. Mass Spectrom. Rev. 24, 661–700. https://doi.org/10.1002/mas.20033

Sotiropoulou, R.E.P., Tagaris, E., Pilinis, C., Anttila, T., Kulmala, M., 2006. Modeling new particle formation during air pollution episodes: Impacts on aerosol and cloud condensation nuclei. Aerosol Sci. Technol. 40, 557–572. https://doi.org/10.1080/02786820600714346

https://doi.org/10.5194/egusphere-2022-1165
Preprint. Discussion started: 14 November 2022

Stewart, G.J., Acton, W.J.F., Nelson, B.S., Vaughan, A.R., Hopkins, J.R., Arya, R., Mondal, A., Jangirh, R., Ahlawat, S., Yadav, L., Sharma, S.K., Dunmore, R.E., Yunus, S.S.M., Nicholas Hewitt, C., Nemitz, E., Mullinger, N., Gadi, R., Sahu, L.K., Tripathi, N., Rickard, A.R., Lee, J.D., Mandal, T.K., Hamilton, J.F., 2021a. Emissions of non-methane volatile organic compounds from combustion of domestic fuels in Delhi, India. Atmos. Chem. Phys. 21, 2383–2406. https://doi.org/10.5194/acp-21-2383-2021

Stewart, G.J., Nelson, B.S., Acton, W.J.F., Vaughan, A.R., Farren, N.J., Hopkins, J.R., Ward, M.W., Swift, S.J., Arya, R., Mondal, A., Jangirh, R., Ahlawat, S., Yadav, L., Sharma, S.K., Yunus, S.S.M., Nicholas Hewitt, C., Nemitz, E., Mullinger, N., Gadi, R., Sahu, L.K., Tripathi, N., Rickard, A.R., Lee, J.D., Mandal, T.K., Hamilton, J.F., 2021b. Emissions of intermediate-volatility and semi-volatile organic compounds from combustion of domestic fuels in Delhi, India. Atmos. Chem. Phys. 21, 2407–2426. https://doi.org/10.5194/acp-21-2383-2021

Stewart, G.J., Nelson, B.S., Drysdale, W.S., Acton, W.J.F., Vaughan, A.R., Hopkins, J.R., Dunmore, R.E., Hewitt, C.N., Nemitz, E., Mullinger, N., Langford, B., Shivani, Reyes-Villegas, E., Gadi, R., Rickard, A.R., Lee, J.D., Hamilton, J.F., 2021c. Sources of non-methane hydrocarbons in surface air in Delhi, India. Faraday Discuss. 226, 409–431. https://doi.org/10.1039/d0fd00087f

Stockwell, C.E., Veres, P.R., Williams, J., Yokelson, R.J., 2015. Characterization of biomass burning emissions from cooking fires, peat, crop residue, and other fuels with high-resolution proton-transfer-reaction time-of-flight mass spectrometry. Atmos. Chem. Phys. 15, 845–865. https://doi.org/10.5194/acp-15-845-2015

Talukdar, S., Tripathi, S.N., Lalchandani, V., Rupakheti, M., Bhowmik, H.S., Shukla, A.K., Murari, V., Sahu, R., Jain, V., Tripathi, N., Dave, J., Rastogi, N., Sahu, L., 2021. Air pollution in new delhi during late winter: An overview of a group of campaign studies focusing on composition and sources. Atmosphere (Basel). 12, 1–22. https://doi.org/10.3390/atmos12111432

Tang, T., Cheng, Z., Xu, B., Zhang, B., Zhu, S., Cheng, H., Li, J., Chen, Y., Zhang, G., 2020. Triple Isotopes (δ13C, δ2H, and Δ14C) Compositions and Source Apportionment of Atmospheric Naphthalene: A Key Surrogate of Intermediate-Volatility Organic Compounds (IVOCs). Environ. Sci. Technol. 54, 5409–5418. https://doi.org/10.1021/acs.est.0c00075

Tobler, A., Bhattu, D., Canonaco, F., Lalchandani, V., Shukla, A., Thamban, N.M., Mishra, S., Srivastava, A.K., Bisht, D.S., Tiwari, S., Singh, S., Močnik, G., Baltensperger, U., Tripathi, S.N., Slowik, J.G., Prévôt, A.S.H., 2020. Chemical characterization of PM2.5 and source apportionment of organic aerosol in New Delhi, India. Sci. Total Environ. 745, 1–12. https://doi.org/10.1016/j.scitotenv.2020.140924

Tripathi, N., Sahu, L., 2020. Chemosphere Emissions and atmospheric concentrations of a -pinene at an urban site of India : Role of changes in meteorology. Chemosphere 256, 127071. https://doi.org/10.1016/j.chemosphere.2020.127071

Tripathi, N., Sahu, L.K., Patel, K., Kumar, A., Yadav, R., 2021. Ambient air characteristics of biogenic volatile organic compounds at a tropical evergreen forest site in Central Western Ghats of India. J. Atmos. Chem. 78, 139–159. https://doi.org/10.1007/s10874-021-09415-y

Tripathi, N., Sahu, L.K., Wang, L., Vats, P., Soni, M., Kumar, P., Satish, R. V., Bhattu, D., Sahu, R., Patel, K., Rai, P., Kumar, V., Rastogi, N., Ojha, N., Tiwari, S., Ganguly, D., Slowik, J., Prévôt, A.S.H., Tripathi, S.N., 2022. Characteristics of VOC composition at urban and suburban sites of New Delhi, India in winter. J. Geophys. Res. Atmos. 1–28. https://doi.org/10.1029/2021jd035342

Ulbrich, I.M., Canagaratna, M.R., Zhang, Q., Worsnop, D.R., Jimenez, J.L., 2009. Interpretation of organic components from Positive Matrix Factorization of aerosol mass spectrometric data. Atmos. Chem. Phys. 9, 2891–2918. https://doi.org/10.5194/acp-9-2891-2009

Uttar Pradesh Pollution Control Board, 2019. Action Plan for the control of Air Pollution in Lucknow city.

Wang, L., Slowik, J., Tripathi, N., Bhattu, D., Rai, P., Kumar, V., Vats, P., Satish, R., Baltensperger, U., Ganguly, D., Rastogi, N., Sahu, L., Tripathi, S., Prévôt, A., 2020. Source characterization of volatile organic compounds measured by PTR-ToF-MS in Delhi, India. Atmos. Chem. Phys. 1–27. https://doi.org/10.5194/acp-2020-11

Wang, L., Slowik, J.G., Tong, Y., Duan, J., Gu, Y., Rai, P., Qi, L., Stefenelli, G., Baltensperger, U., Huang, R.J., Cao, J., Prévôt, A.S.H., 2021a. Characteristics of wintertime VOCs in urban Beijing: Composition and source apportionment. Atmos. Environ. X 9. https://doi.org/10.1016/j.aeaoa.2020.100100

https://doi.org/10.5194/egusphere-2022-1165
Preprint. Discussion started: 14 November 2022

Wang, L., Slowik, J.G., Tong, Y., Duan, J., Gu, Y., Rai, P., Qi, L., Stefenelli, G., Baltensperger, U., Huang, R.J., Cao, J., Prévôt, A.S.H., 2021b. Supplement for: Characteristics of wintertime VOCs in urban Beijing: Composition and source apportionment. Atmos. Environ. X 9, 2–6. https://doi.org/10.1016/j.aeaoa.2020.100100

Wang, S., Newland, M.J., Deng, W., Rickard, A.R., Hamilton, J.F., Muñoz, A., Ródenas, M., Vázquez, M.M., Wang, L., Wang, X., 2020. Aromatic Photo-oxidation, A New Source of Atmospheric Acidity. Environ. Sci. Technol. 54, 7798–7806. https://doi.org/10.1021/acs.est.0c00526

WHO, 2021. IARC Monographs on the identification of carcinogenic hazards to Humans.

Yee, L.D., Kautzman, K.E., Loza, C.L., Schilling, K.A., Coggon, M.M., Chhabra, P.S., Chan, M.N., Chan, A.W.H., Hersey, S.P., Crounse, J.D., Wennberg, P.O., Flagan, R.C., Seinfeld, J.H., 2013. Secondary organic aerosol formation from biomass burning intermediates: Phenol and methoxyphenols. Atmos. Chem. Phys. 13, 8019–8043. https://doi.org/10.5194/acp-13-8019-2013

Zhang, Q., Jimenez, J.L., Canagaratna, M.R., Ulbrich, I.M., Ng, N.L., Worsnop, D.R., Sun, Y., 2011. Understanding atmospheric organic aerosols via factor analysis of aerosol mass spectrometry: A review. Anal. Bioanal. Chem. 401, 3045–3067. https://doi.org/10.1007/s00216-011-5355-y

Zhang, Z., Wang, H., Chen, D., Li, Q., Thai, P., Gong, D., Li, Y., Zhang, C., Gu, Y., Zhou, L., Morawska, L., Wang, B., 2017. Emission characteristics of volatile organic compounds and their secondary organic aerosol formation potentials from a petroleum refinery in Pearl River Delta, China. Sci. Total Environ. 584–585, 1162–1174. https://doi.org/10.1016/j.scitotenv.2017.01.179

https://doi.org/10.5194/egusphere-2022-1165
Preprint. Discussion started: 14 November 2022

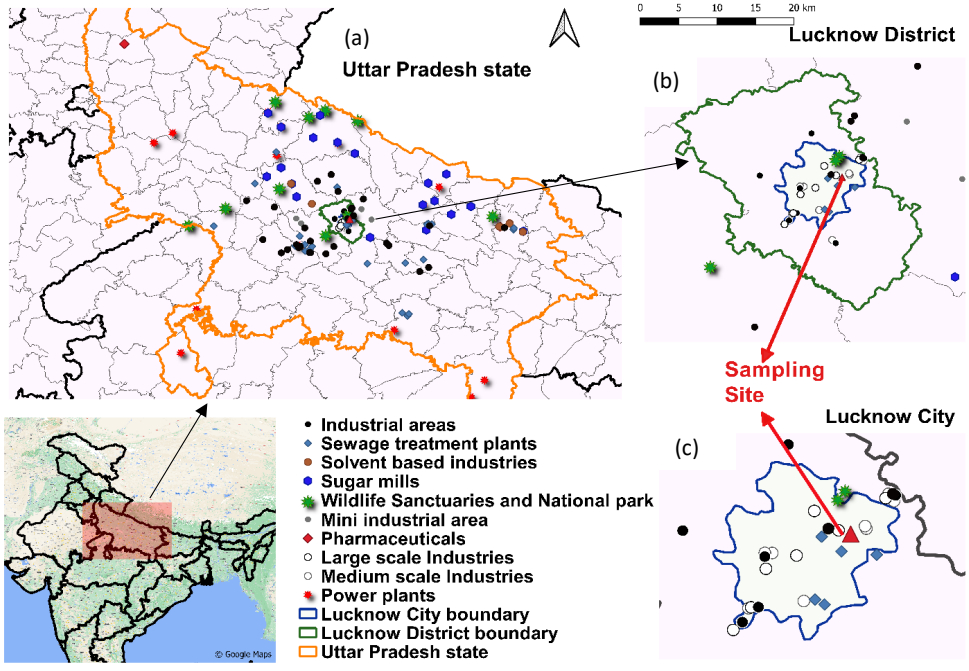

Figure 1: Detailed map of (a) Uttar Pradesh state , (b) Lucknow district and (c) Lucknow city with highlighted sampling site and major potential point-sources of NMVOCs

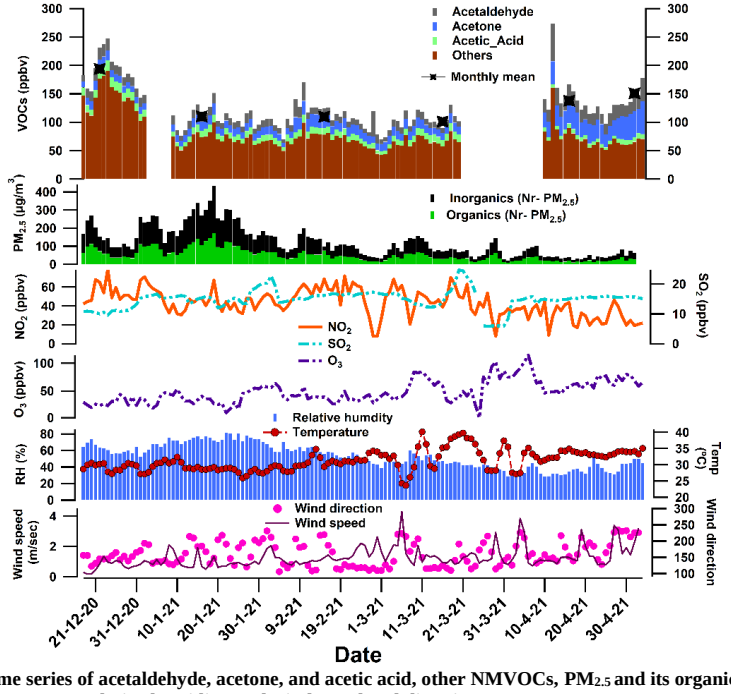

Figure 2: Time series of acetaldehyde, acetone, and acetic acid, other NMVOCs, $PM_{2.5}$ and its organic fraction, NO_2, SO_2, O_3, temperature, relative humidity, and wind speed and direction

https://doi.org/10.5194/egusphere-2022-1165
Preprint. Discussion started: 14 November 2022

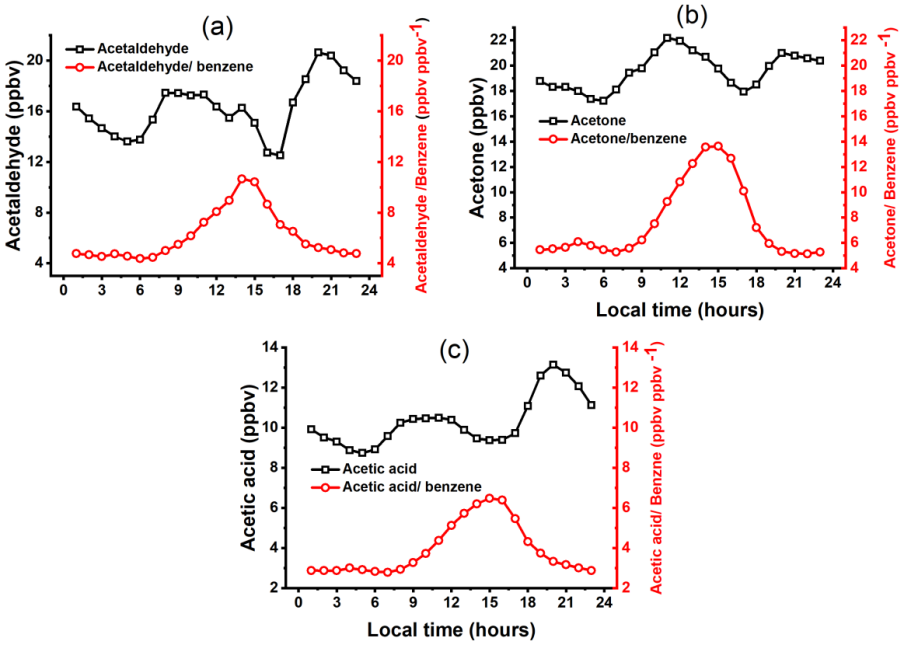

Figure 3: Diurnal variations over the whole study period for (a) Acetaldehyde and Acetldehyde/benzene ratio, (b) Acetone and Acetone/benzene ratio, and (c) Acetic acid and Acetic acid/benzene ratio

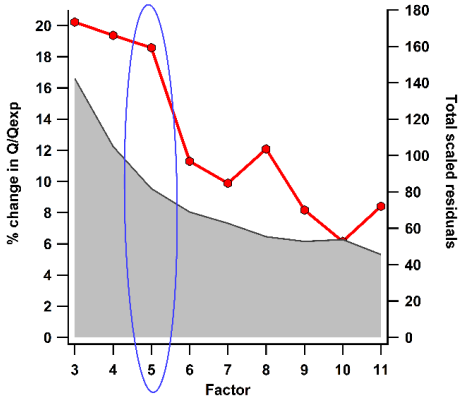

Figure 4: The Q/Qexp plot (% change) and total summed scaled residuals for each factor solution

https://doi.org/10.5194/egusphere-2022-1165
Preprint. Discussion started: 14 November 2022

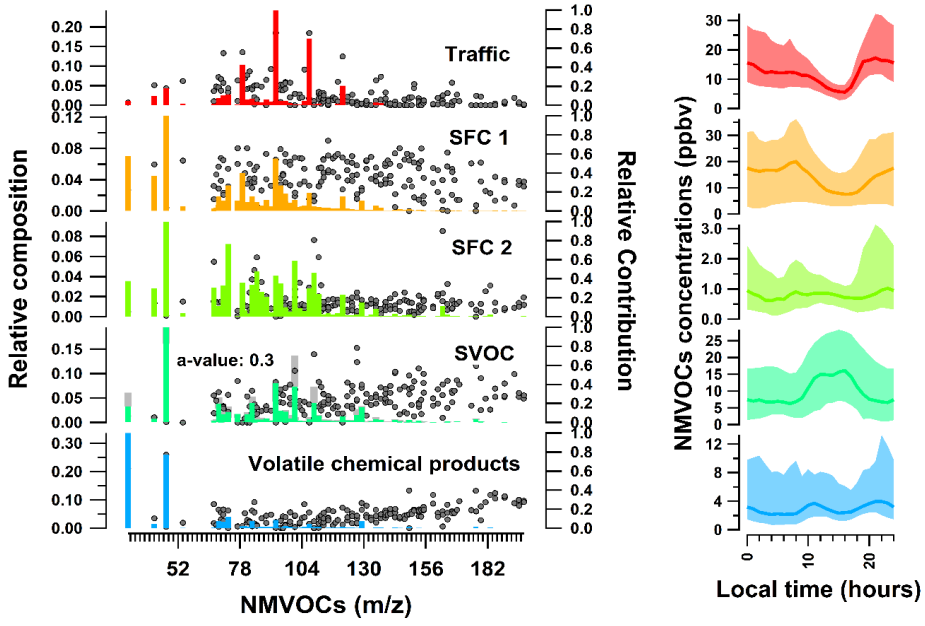

Figure 5: Profile and diurnal variation of individual factors of selected 5-factor solution after PMF analysis

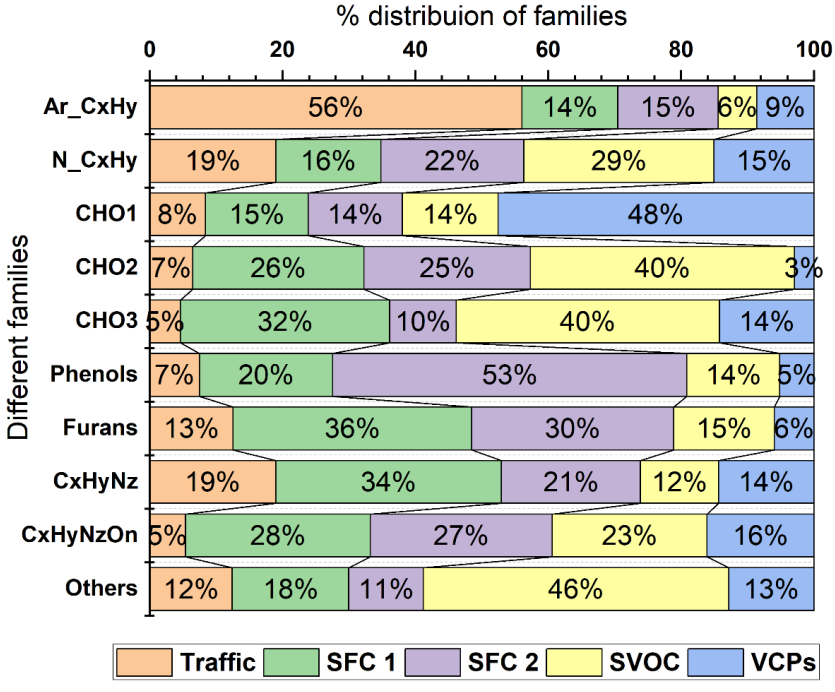

Figure 6: Relative contributions (%) of different families to the individual factors

https://doi.org/10.5194/egusphere-2022-1165
Preprint. Discussion started: 14 November 2022

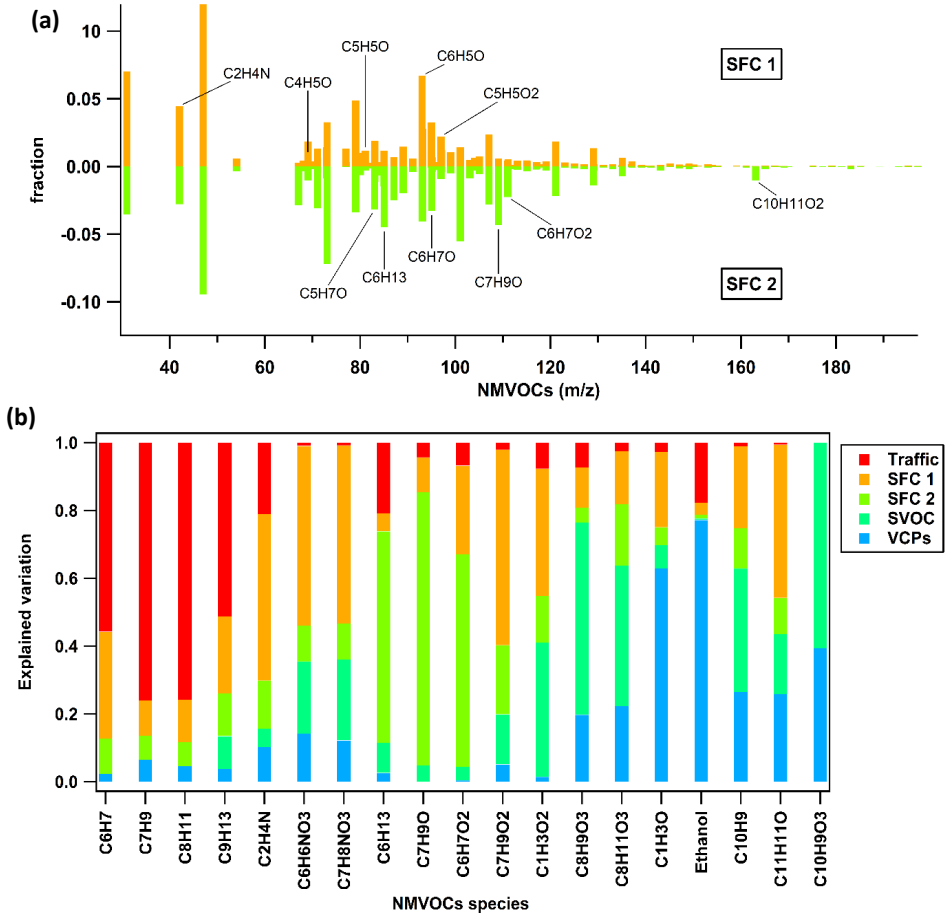

Figure 7: (a) Comparison of relative composition of two factor profiles (SFC 1 and SFC 2). SFC 1 spectrum on top and SFC 2 spectrum on bottom. (b) Explained variation of selected NMVOCs species, stacked such that total explained variation is 1, colour coded by the five factors.

https://doi.org/10.5194/egusphere-2022-1165
Preprint. Discussion started: 14 November 2022

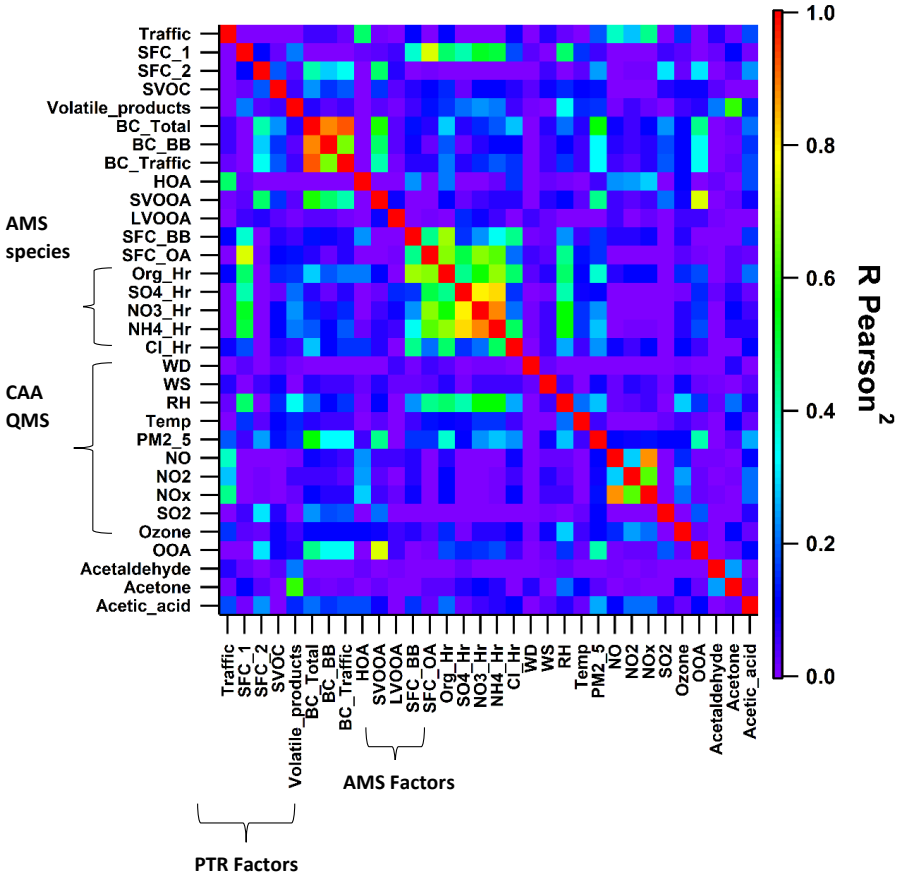

Figure 8: Corelation of the five factors to the external measurements, including factors from AMS, Organics NR-$PM_{2.5}$ and Inorganics NR-$PM_{2.5}$, Black carbon (BC total, % BC from fossil and non-fossil fuels), CAAQMS data, total oxygenated organic aerosols (OAA), VOCs species. The CAAQMS data includes wind direction (WD), wind speed (WS), relative humidity (RH), ambient temperature (Temp), Particulate matter (PM2.5), nitric oxide (NO), nitrogen dioxide (NO_2), nitrogen oxides (NO_X), sulphur dioxide (SO_2) and Ozone. The correlation between the timeseries of the parameters is represented by R Pearson^2, colour coded with rainbow color scheme, showing violet as 0 (no correlation) and red as 1 (highest correlation).

https://doi.org/10.5194/egusphere-2022-1165
Preprint. Discussion started: 14 November 2022

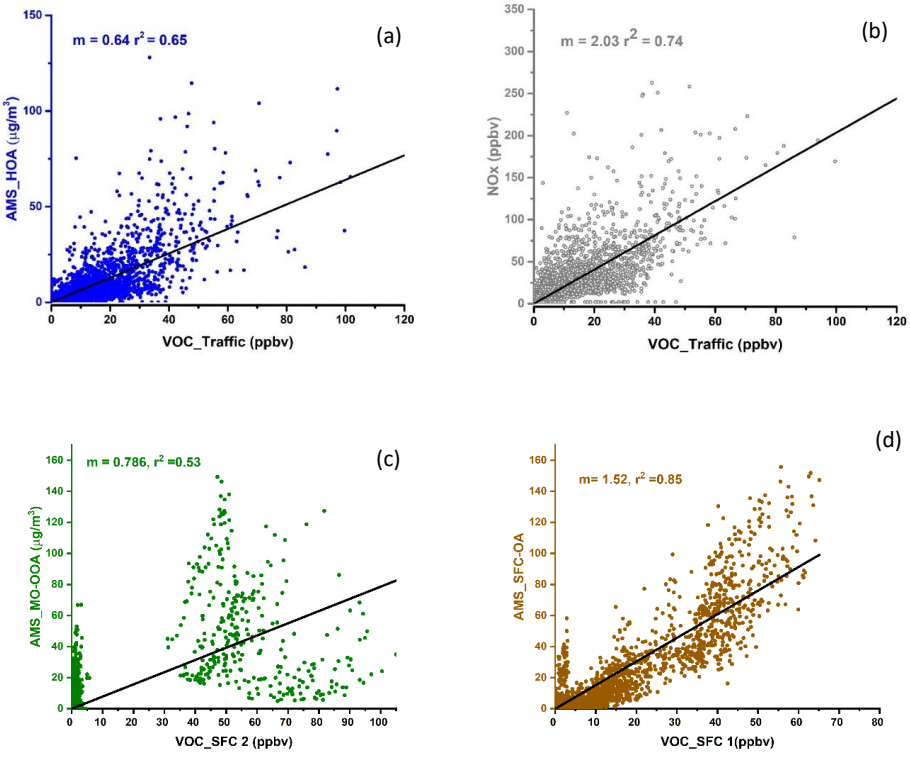

Figure 9: Scatter plots showing a correlation between VOC_factors with their respective AMS_factors

https://doi.org/10.5194/egusphere-2022-1165
Preprint. Discussion started: 14 November 2022

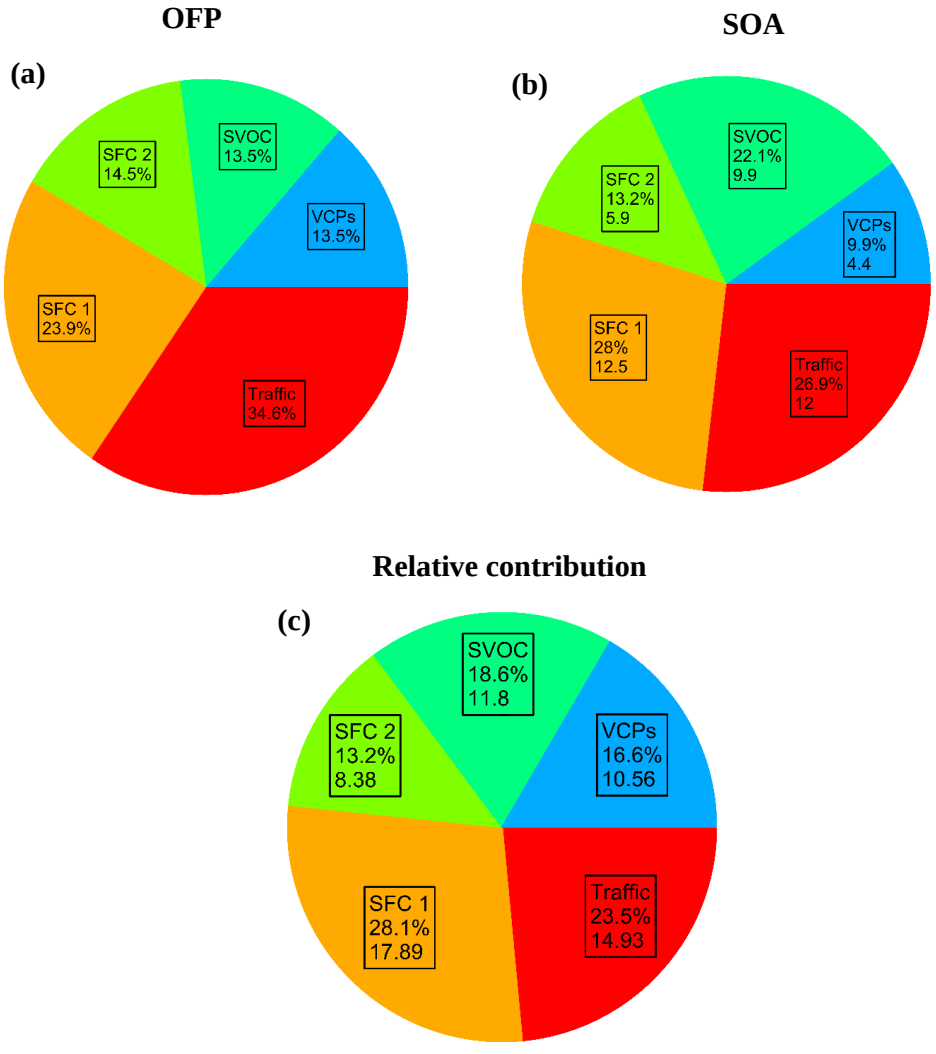

Figure 10: Distribution of individual factors to (a) Ozone formation potential (OFP), (b) SOA formation, (c) Relative contribution